Flash Photolysis of Sensitizers in Microbes†

Timothy C. Oldham and David Phillips*

Department of Chemistry, Imperial College of Science, Technology and Medicine, South Kensington, London SW7 2AY, U.K.

Received: April 30, 1999; In Final Form: August 1, 1999

Spectroscopic and physiological studies of the photoinactivation of oral microbes suggest that there is no single mechanism of photodynamic cell kill operating in all microbes. It is proposed that the photoinactivation of *Streptococcus mutans* (a Gram-positive bacterium) requires only the generation of $^1O_2$, whereas the photoinactivation of both *Porphyromonas gingivalis* (a Gram-negative bacterium) and *Candida albicans* (a yeast) requires a contribution from another mechanism, most likely a type I electron transfer mechanism involving the photosensitizer. The type I process seems to initiate changes in the permeability of the cell wall of *P. gingivalis* and *C. albicans* which permit the sensitizers and probably $^1O_2$ access to intracellular targets. The hypothesis is supported by new work described here as well as a considerable body of independent data.

Introduction

A wide range of microbes (bacteria, yeasts, viruses, fungi, paramecia, etc) have been shown to be susceptible to photosensitized inactivation.[1−6] Less detail has been published concerning the mode of inactivation, and the majority of this focuses on physiological rather than photochemical mechanisms.

The relevant photophysics of sensitizers is summarized in Figure 1. Essentially, there are two possibilities, that of energy transfer from the excited triplet state of a sensitizer to ground state oxygen to produce $O_2(^1\Delta_g)$ as a cytotoxic species (type II process); and a radical process (type I), initiated by electron transfer from an excited state. The present work was undertaken to attempt to resolve the photochemical mechanism of microbe death for a variety of microbes using flash photolysis and steady-state photophysical techniques.

The wide acceptance of the type II $^1O_2$ pathway as the dominant mode of action stems from the observation of efficient $^1O_2$ generation by most effective sensitizers and extensive use of $^1O_2$ quenchers and traps in vivo. The latter results tend to be ambiguous since few probes are specific for $^1O_2$[7−9] and the high concentrations of quenchers required are likely to distort the system. Many studies address only one or other pathway, usually the type II process.

A number of more rigorous indirect studies[10−17] suggest a variety of fates for initial excitation energy, but cannot probe the initial dark reaction.

Loss of photosensitizing action upon exclusion of oxygen cannot unequivocally implicate the $^1O_2$ mechanism since oxygen may propagate radical reactions initiated by type I processes, or even take part in electron transfer to form superoxide ($O_2^{\bullet-}$). Correlation of cell kill with solution phase quantum yields of singlet oxygen production (Φ_Δ) is equally limiting since in solution Φ_Δ is usually the same or very close to the triplet quantum yield (Φ_T). The best that can be said in such a case is the cell kill is definitely mediated by the sensitizer triplet state. The behavior of sensitizers in vivo may, however, be vastly different from that in vitro.[18]

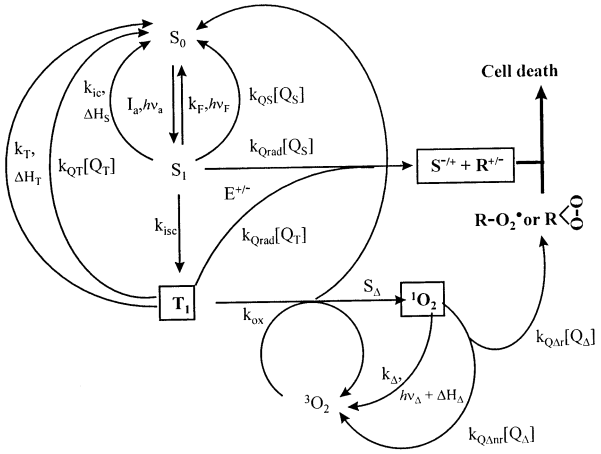

Figure 1. Photophysics and photochemistry of photodynamic action. S and T represent the singlet and triplet states of the sensitizer, respectively. k_i represents a rate constant for the processes indicated by i as follows: F = fluorescence, a = absorption, ISC = intersystem crossing, IC = internal conversion, ox = quenching of the triplet state by oxygen, Δ = nonradiative (solvent assisted) and radiative decay of $^1O_2$, T = nonradiative (intersystem crossing) deactivation of the triplet state; Q_j = quenching by process j (Δ_r and Δ_{nr} are reactive and nonreactive quenching of $^1O_2$ by quencher Q_Δ, rad = electron transfer quenching of the triplet by Q_T, S = energy transfer quenching of the singlet state by Q_S, T = energy transfer quenching of the triplet state by Q_T. ΔH_k indicates that state k (S = singlet, T = triplet, Δ = $^1O_2$) releases heat during the decay process. $h\nu_m$ indicates that a photon is absorbed or emitted by the process (a = absorption, F = fluorescence from the singlet state, Δ = luminescence from $^1O_2$). S_Δ is the fraction of triplet states quenched by oxygen which yield $^1O_2$. $E^\pm$ is the set of redox potentials governing the reaction of the singlet or triplet states. Species in boxes were monitored in the present work.

The exact processes by which initial excitation energy translates into observed physiological effects, and particularly the fraction of that initial energy which is diverted between competing processes, can be determined using direct spectroscopic studies of sensitizer photophysics "on location" inside cells. All the key intermediates (sensitizer singlet and triplet states and radical ions as well as singlet oxygen) are in principle spectroscopically identifiable. Temporal resolution enables the triplet decay to be correlated with the growth of its products.

† Paper for special edition of *J. Phys. Chem.* in honor of the 65th birthday of J. K. Thomas.

* To whom correspondence should be addressed.

10.1021/jp991438s CCC: $18.00 © 1999 American Chemical Society
Published on Web 09/17/1999

TABLE 1: Photoinactivation of Oral Pathogens in Saline Suspensions by the Sensitizers TB and AlPcS2[a]

	[dye]/μg mL^{-1}	[cells][b]/ cfu mL^{-1}	laser[c]	irradiation time/s	log cell kill[d]	ref
S. mutans						
$AlPcS_2$	50	2×10^7	GaAlAs	90	0.8	*e*
	50	1×10^7	GaAlAs	60	2.8	*f*
	25	3×10^6	GaAlAs	240	>4	*g*
TB	50	7×10^6	He/Ne	90	>0.65[n]	*h*
	25	3×10^6	He/Ne	240	>4	*g*
P. gingivalis						
$AlPcS_2$	25	3×10^8	He/Ne	80	1.8	*i*
TB	25	5×10^7	He/Ne	5	>3	*j*
	50	plaque[o]	He/Ne	30	>3	*k*
C. albicans						
$AlPcS_2$	100	2×10^5	GaAlAs	120	0[n]	*l*
TB	100	3×10^5, 6×10^6	He/Ne	120	0.5[n]	*l, m*

[a] Where a range of conditions was used in a given reference, only the minimum sensitizer and power conditions used to achieve maximum kill are listed. [b] Cells suspended in PBS containing sensitiser and irradiated. [c] He/Ne = continuous wave helium neon laser at 632.8 nm delivering 550 m W cm^{-2} in a 1.3 mm diameter beam. GaAlAs = pulsed (20 kHz) gallium aluminium arsenide laser diode at 660 nm delivering 17 mW cm^{-2} in a 9 mm diameter beam at the sample. [d] Cell kills are conventionally expressed in log units. Thus a cell population reduced from 10^9 to 10^4 cfu mL^{-1} is said to have undergone a 5 log reduction. [e] Burns, T., Wilson, M., Pearson, G. J. *J. Dent.* **1994**, *22*, 273. [f] Wilson, M. personal communication. [g] Burns, T., Wilson, M. and Pearson, G. J. SPIE Proc. **1995**; *2625*, 288. [h] Burns, T., Wilson, M. and Pearson, G. J. *J. Med. Microbiol.* **1993**, *38*, 401. [i] Wilson, M., Dobson, J. and Sarkar, S. *Oral Microbiol. Immunol.* **1993**, *8*, 182. [j] Wilson, M. and Dobson, J. *Clin. Infect. Diseases* **1993**, *16*, S414. [k] Sarkar, S. and Wilson, M. *J. Periodont. Res.* **1993**, *28*, 204. [l] Wilson, M. and Mia, N. *J. Oral. Pathol. Med.* **1993**, *22*, 354. [m] Wilson, M. and Mia, N. *Lasers Med. Sci.* **1994**, *9*, 105. [n] Some dark toxicity was observed. Cell kills are corrected for dark toxicity. [o] Plaque samples from patients, when suspended in PBS yielded 10^2-10^5 cfu mL^{-1}.

The strategy adopted in this work was to use spectroscopy to search systematically for sensitizer triplet states, radical ions, and singlet oxygen in suspensions of a range of cell types. Limited photophysical studies on cell suspensions have been conducted previously, and these demonstrate the feasibility of detecting spectroscopically triplet states and singlet oxygen in such systems.[19−29]

Microbes Studied. *Streptococcus mutans*, a Gram-positive bacterium believed to be a primary agent responsible for dental caries formation, *Porphyromonas gingivalis*, a Gram-negative bacterium believed to be the prime causative agent of periodontitis, and *Candida albicans*, a yeast of major importance in HIV-associated oral candidosis, were chosen for detailed study. The selection was based upon their importance as oral pathogens, and availability of physiological data and the range of microbial structures they represent. Some work was also conducted with *Escherichia coli* due to repeated claims that it and other Gram-negative bacteria cannot be inactivated photodynamically.[30−32]

The microbes and sensitizers were selected on the basis of previous work which established sensitivity to cell kill, and whether cells took up the sensitizer. The available data on the photoinactivation of oral pathogens in saline suspensions is summarized in Table 1, from which it can be seen that the efficacy of both toluidine blue, TB, and disulfonated aluminum phthalocyanine, $AlPcS_2$, against different organisms follows the series: *S. mutans* > *P. gingivalis* > *C. albicans*. $AlPcS_2$ is more effective against *S. mutans*, while TB is more effective against the other organisms under the conditions used. Both TB and $AlPcS_2$ are taken up strongly by *S. mutans* and TB is also taken up by *P. gingivalis*. Neither sensitizer is taken up by *C. albicans*.

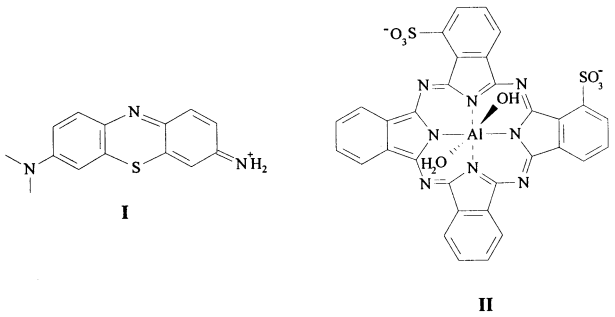

I **II**

Figure 2. Structure of TB (**I**) and $AlPcS_2$ (**II**) used in this work. The α,α-isomer of $AlPcS_2$ shown is believed to be the dominant component of the "clinical" $AlPcS_2$ preparation used. Both dyes are shown in the form in which they are believed to exist in aqueous solution at pH 7 (see below).

Where it occurs, sensitizer uptake is extremely rapid. Maximum intracellular concentrations are reached in less than 1 min for TB absorption *by P. gingivalis*[33] and thiopyronine absorption by *Proteus mirabilis*.[34] The localization of sensitizers within the microbial cells is not well-known. Although TB (in common with other cationic dyes) is capable of inducing DNA strand breaks, it does not bind to DNA in *P. gingivalis*. Radio-labeling studies of cell fractions have shown that under typical photosensitization conditions 90−% of the dye locates in the outer membrane, with the remaining 10% believed to locate in the cytoplasm.[33] Zinc phthalocyanines (neutral and sulfonated) appear to localize in the cytoplasmic membrane (80−90%) and the outer membrane (10−20%) of *E. coli*.[31]

Species differences in the cell wall are likely to be at least partly responsible both for differences in cell killing efficiency and for differential sensitizer uptake between different types of organism and different sensitizers. Indeed, lack of uptake may be the basis for numerous assertions that photosensitization will not inactivate Gram-negative bacteria,[32−34] although the observation that *P. gingivalis* can be inactivated by both TB and $AlPcS_2$ suggests the problem is more than simply one of localization. It has been shown that sensitizer uptake is species-dependent rather than Gram-type dependent and is influenced by sensitizer charge.[35,36] The lower sensitivity of *C. albicans* may also be attributed to its larger size if it can be assumed that a certain level of intracellular damage is required to kill each cell.

S. mutans cell kill is enhanced when D_2O saline replaces H_2O saline. Complete or almost complete survival is observed when oxygen is excluded or in the presence of 0.1 M methionine or 0.5 M NaN_3. The protection afforded by methionine and NaN_3 is dose dependent. As cell kill increases, increased levels of intracellular material are detected in the medium and lipid peroxidation products levels increase. Kills of *P. gingivalis* are also enhanced in D_2O and are inhibited by L-tryptophan.[37] Such studies are suggestive of a key role for $^1O_2$.

Type II processes alone do not seem to be able to account for all the mechanistic observations. Kills of *C. albicans* by TB are pH dependent: at pH 4.0 they are 85% of those at pH 7.0.[38] Since the quantum yield of $^1O_2$ production by TB falls 60% from 0.6 at pH 7.0 to 0.25 at pH 4.5,[39] these results suggest that while $^1O_2$ does contribute to inactivation, there is a significant contribution from other mechanisms. The present work was undertaken to investigate these mechanisms further.

Sensitizers. The sensitizers studied here were toluidine blue (I) and disulfonated aluminum phthalocyanine (II), Figure 2.

Toluidine blue is a thiazine dye, belonging to the same family as thionine (the parent dye of the family) and methylene blue.

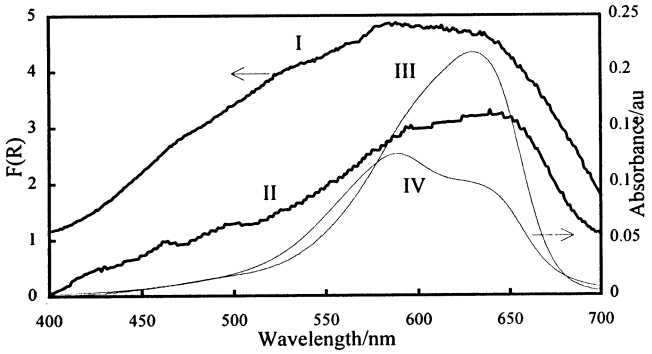

Figure 3. Absorption spectrum of TB in complex media. (I) Ground state remission spectrum F(R) of TB bound to sepharose beads recorded with a black background (the background remission spectrum of the beads has been subtracted). (II) Corrected absorption spectrum (on an arbitrary scale) of TB in *P. gingivalis*. Also shown are absorption spectra (normalized by concentration) of TB in PBS at 1.1 μM (III) and 57 μM(IV).

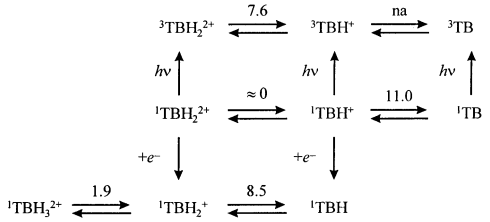

Figure 4. Acid−base properties of TB. Values are pK_a's (after Tuite and Kelly[6]).

Its photophysics and photochemistry were recently reviewed by Tuite and Kelly.[6] The ground state absorption spectrum in aqueous solution displays a maximum at 630 nm with a distinct concentration dependent shoulder due to absorption of the aggregate (probably a face-to-face dimer) at 585−590 nm (see Figure 3). The dimerization constant of the related methylene blue is 6×10^3 M^{-1} and increases with ionic strength. Unlike $AlPcS_2$, the rate of reequilibration in toluidine blue following a change in concentration is rapid. TB is also metachromatic, i.e., the position of the absorption band is dependent upon the substrate to which it is bound. When bound to DNA, the band is near 645 nm, while in 1% agar, the band may be displaced as far as 540 nm.[40] The ground state extinction coefficient in ethanol is 63 000 M^{-1} cm^{-1}.[40]

The acid-based and electrochemical properties of TB are important and are summarized in Figure 4. The monocation is the stable ground species under most conditions. The fluorescence quantum yield was determined to be 0.025 ± 0.003 in PBS over the range pH 5.9−7.2, in good agreement with a value of 0.029 determined for thionine.[41] The fluorescence lifetime was found to be monoexponential in alcoholic solvents with a lifetime of 450−500 ps. In aqueous solution the decay was biexponential with the main component at 240−250 ps and a minor component (10−15%) at 420−450 ps (cf 370 ps for MB). The minor component may be due to dimer, although the dimer is said to be nonfluorescent.[6]

In the triplet state at physiological pH both the monocation and the protonated dication will be present. The lifetime of the dicationic protonated triplet state is 5 μs in the absence of oxygen (a similar value was measured in the present work) and it is quenched by oxygen with a rate constant of 2.9×10^8 M^{-1} s^{-1}. The monocationic triplet lifetime was found to be 58 μs in oxygen-free water in good agreement with a value of 60 μs measured elsewhere,[39] although it was found to be considerably shorter in PBS. The monocationic triplet is quenched by oxygen with a rate constant of 3.3×10^9 M^{-1} s^{-1}.[39] This gives rise to a pH-dependent triplet quantum yield varying from 0.25 at pH 5 to 0.9 at pH 9 in air-saturated water. The triplet−singlet difference absorption spectra shown later are in good agreement with the triplet spectrum of thionine,[41] though the low pH spectrum seems to include a contribution from the monocationic species as well as the protonated dication. The triplet extinction coefficients are low: 13 500 M^{-1} cm^{-1} at 365 nm and 15 500 M^{-1} cm^{-1} at 690 nm for the dication and 12 000 M^{-1} cm^{-1} at 420 nm and 9 000 M^{-1} cm^{-1} at 800 nm for the monocation assuming that the values are similar to those for thionine.[41] The triplet energies have been estimated at 12 600 cm^{-1} for the monocation and 900 cm^{-1} for the protonated dication.[39] A comparison of the ground state absorption spectrum and the excited state singlet depletion spectrum suggests that the dimer does not generate triplet states.

TB is readily reduced from both ground and excited states. The reduced or leucoform of the dye is colorless. Evidence for the products of the electron transfer quenching of thionine and methylene blue triplet states has been obtained using EDTA and *N*,*N*,*N*′,*N*′-tetramethylphenylenediamine as reductants. The protonation of the ring nitrogen (i.e., to form the dication) increases the rate of electron transfer by a factor of 20, while the neutral form of the dye cannot be reduced by EDTA. Methylation of the amino side groups, as in TB, reduces the rate slightly.[42,43] Reduction is inhibited or rapidly reversed by oxygen yielding H_2O_2 or $O_2^{\bullet-}$ which are further potential initiators of oxidative damage.[6] Of importance to quenching studies is the observation that azide quenches thionine triplet states in water with a rate constant of 1.8×10^8 M^{-1} s^{-1}, increasing to 1.6×10^9 M^{-1} s^{-1} in methanol.[44]

The ground state absorption spectrum of $AlPcS_2$ in aqueous solution is characterized by a sharp Q-band absorption at 673 nm and usually additional absorption in the range 570−850 nm which is attributed to aggregate absorption (see Figure 6). Aggregation is enhanced in PBS. The rate of adjustment of the aggregate−monomer equilibrium to changes in concentration is very slow and proceeds on a time scale of hours. The aggregate is thought to be nonfluorescent and nonphotoactive.[45] The fluorescence lifetime and quantum yield of the monomer in PBS are 5 ns and 0.40, respectively.[46,47] The triplet spectrum is characterized by a broad absorption peaking at 490 nm with an extinction coefficient of 36 000 M^{-1} cm^{-1}.[47] The lowest triplet energy level should be 9 000−9 500 cm^{-1} above the ground singlet state, assuming a value similar to that for zinc phthalocyanines.[48] The quantum yield of triplet formation was found to be 0.22 in H_2O falling to 0.15 ± 0.02 in PBS over the range pH 5.9−7.2, in good agreement with previous determinations.[46,47] Recently, the pH dependence of the triplet state properties has been investigated.[49] The triplet lifetime, quantum yield, and singlet oxygen quantum yield all display a sharp decrease in the region of pH 7, with the triplet lifetime falling from 450 to 500 μs in oxygen-free PBS to 300−350 μs as the pH decreases from pH 8 to pH 4. This has been attributed to changes in the protonation of the water ligands on the metal center.[50]

The microbes studies included both *procaryotic* (without intracellular membranes and thus without defined organelles) bacteria, and *eucaryotic* (with intracellular structure and membranes) yeast. In a procaryotic cell, the single DNA strand is not constrained to a defined nucleus, and many cellular functions take place at the cell surface rather than in the distinct organelles of a eucaryotic cell. The interior of a procaryotic

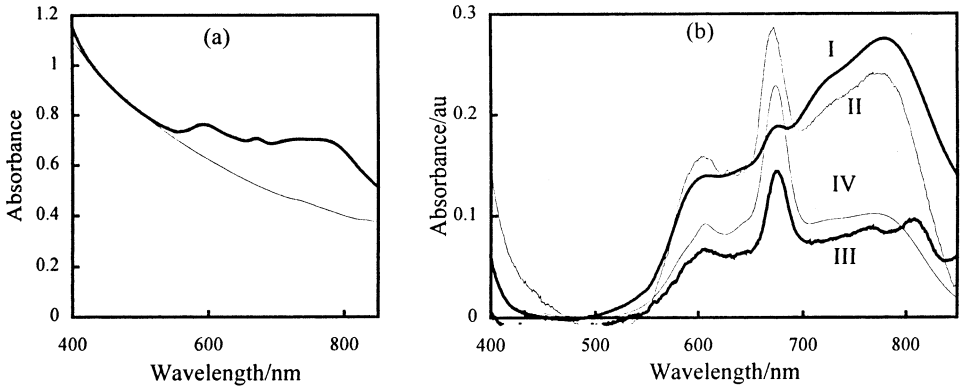

Figure 5. Corrected absorption spectra of $AlPcS_2$ in a variety of cell systems: (a) uncorrected spectrum of $AlPcS_2$ in *S. mutans* whole cells showing scaled background; (b) corrected spectra for $AlPcS_2$ in (I) *S. mutans* (the spectrum in *S. mutans* protoplasts was identically shaped), (II) *C. albicans* spheroplasts, (III) P1.HTR cells and for comparison (IV) PBS at 18 μg mL^{-1} (24 μM).

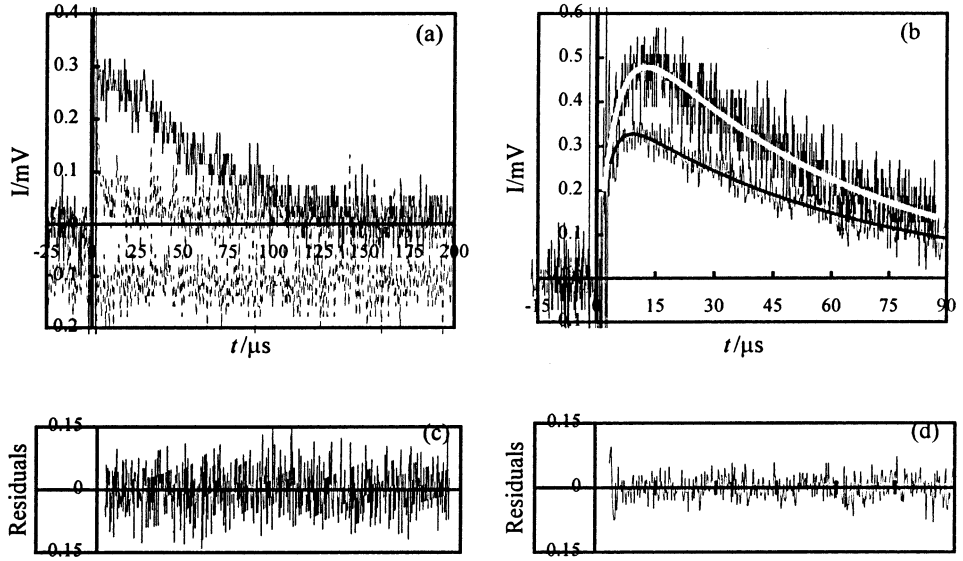

Figure 6. Time-resolved near-IR luminescence at 1270 nm from TB immobilized on sepharose beads in D_2O/NaCl. Beads contained 5.5 $\pm$ 0.3 μg mL^{-1} TB. Excitation was 0.49 mJ pulse^{-1} at 635 nm and the decays are the average of 64 shots. (a) Beads suspended in 7 volumes of D_2O/NaCl. Dashed line is the signal in argon purged solvent. The offset dashed line is the signal from filtered supernatant (offset 0.1 mV for clarity). (b) White fit: beads suspended in 3 volumes D_2O/NaCl, with argon-purged signal subtracted; black fit: TB in D_2O/NaCl. Lines are fits to eq 7 giving the residuals in (c) (A = 0.65 mV, τ_1 = 4.6 μs, τ_2 = 56.4 μs, χ^2 = 0.70) and (d) (A = 0.40 mV, τ_1 = 2.8 μs, τ_2 = 60.8 μs, χ^2 = 1.22, respectively.

cell, the cytoplasm, is densely packed with ribosomes. Procaryotes metabolize at 10−100-fold higher rates than eurcaryotes. With few exceptions, procaryotic cells are bounded by a cell wall which is often a complex structure.

The innermost structure in both Gram-positive and Gram-negative bacteria is the cytoplasmic membrane. This is a lipid bilayer approximately 8 nm thick comprising phospholipid, glycolipid, and a variety of proteins. The cytoplasmic membrane performs many of the functions of specialist organelles in eucaryotic cells, including metabolite transport into and out of the cell, oxidative phosphorylation, cell wall synthesis, phospholipid synthesis, and secretion of extracellular enzymes and proteins. The differences between Gram-positive and Gram-negative species arise in the structure of the cell wall which forms outside the cytoplasmic membrane.

The Gram-positive cell wall is a largely homogeneous layer of peptidoglycan (*murein*) 20−50 nm thick. Peptidoglycan is a linear copolymer of alternating *N*-acetylglucosamine and *N*-acetylmuramic acid which is relatively species independent. A tetrapeptide (occasionally tripeptide) chain (L-alanine (sometimes glycine or L-serine)−D-glutamic acid−L-diamino acid−D-alanine) is attached to the muramic acids. Adjacent chains are cross-linked via the diamino acid which varies considerably between species but is most frequently L-lysine, diaminopimelic acid, L-diaminobutyric acid, or L-ornithine. The amino acid content and length of the cross-links varies considerably from species to species. The cross-linking may be as high as 100% (e.g. in *Staphylococcus aureus*) and is believed to give rise to the structural rigidity of the Gram-positive cell wall.

A unique feature of Gram-positive bacterial cell walls is the presence of teichoic acids which in some cases may make up 50% of the cell wall. These are polymers of glycerol phosphate or ribitol phosphate with a variety of sugars, amino sugars, or amino acids condensed to the hydroxyl groups. These polymers are covalently linked to either peptidoglycan in the cell wall or a glycolipid in the cytoplasmic membrane and often extend beyond the cell wall. Teichoic acids are antigenic and often strain specific. The peptidoglycan layer usually contains other polysaccharides based on neutral sugars (chiefly rhamnose) and a range of accessory polymers and proteins.

The Gram-positive cell wall is relatively porous, with molecular weight exclusion limits of 60 000−120 000. The cell wall of Gram-negative bacteria is thinner (10−15 nm) and is bounded by an outer membrane. This resembles the cytoplasmic

membrane in many ways, and, unlike the Gram-positive cell wall, forms a significant barrier to the passage of macromolecules and certain small molecules. The outer membrane is potenially more prone to oxidative damage than the cytoplasmic membrane since it has a higher protein:phospholipid content than the cytoplasmic membrane. *Porin* proteins regulate access of hyrophilic solutes to the cytoplasmic membrane via a molecular sieve action. Within the lipid fraction, the ratio of phosphatidylethanolamine to both phosphatidylglycerol and cardiolipin is higher in the outer membrane than the cytoplasmic membrane. Most of the lipid and polysaccharide content of the outer membrane is made up of lipopolysaccharide (LPS) which is not found in Gram-positive bacteria. The majority of the LPS is located on the outer surface of the membrane where it displays antigenic properties and serves a protective function. LPS has a complex structure with considerable species and even strain variation both in overall size and in fine structure.

Between the outer membrane and the cytoplasmic membrane is a region known as the periplasmic space. It contains a thin ($\approx$2 nm) layer of peptidoglycan which is less extensively cross-linked than in Gram-positive bacteria (30% for *E. coli*), and therefore is probably not solely responsible for Gram-positive cell rigidity. The diamino acid is always diaminopimelic acid and the cross-linking is usually a direct peptide bond between this and the terminal D-alanine. In addition to the peptidoglycan sheet, the periplasmic space is probably filled with a gel of highly hydrated peptidoglycan with low cross-linkage.[60] Lipoproteins covalently link the outer membrane to the peptidoglycan monolayer. Lipopolysaccharides and ionic interactions bind the peptidoglycan layer to the cytoplasmic membrane.

The cell wall of yeasts is up to 300 nm thick and appears structurally similar to that of Gram-positive bacteria (it also stains Gram-positive), although it does not contain peptidoglycan, the main constituent of the Gram-positive cell wall. 80% of the dry weight of most cell walls is made up of three polysaccharides. *Glucan* (a branched glucose polymer) and *chitin* (an unbranched *N*-acetyl-D-glucosamine polymer similar to the carbohydrate backbone of peptidoglycan) are skeletal polymers, with the interstitial volume filled with *mannan* (a branched mannose polymer) covalently linked to proteins (mannoproteins). 10% of the cell wall comprises proteins, of which the mannoproteins are the most significant (they are the main antigenic components of the *C. albicans* cell wall). Yeast cell wall lipid contents are generally low (<10%).

On the basis of the known photophysics of these two sensitizers, and the effect upon the microbes chosen, the more detailed spectroscopic and time-resolved studies outlined below were undertaken.

Experimental Section

Ground State Studies. Ground state absorption spectra of the sensitizers incorporated into various cell types were obtained by measuring the absorption of both sensitized and unsensitized cell suspensions. The *apparent* absorption of the unsensitized cells was assumed to be due to scattering only (valid for $\lambda >$ 400) nm for all cells except *P. gingivalis*). The unsensitized background was scaled uniformly so that its absorbance matched that of the sensitized sample in a region where the sensitizer was known not to absorb (typically 500 nm for $AlPcS_2$ and 900 nm for TB). Subtraction of the background from the sensitized cell spectrum yielded an approximate absorption spectrum for the cell bound sensitizer. Extinction coefficients were not strictly comparable between samples; however, the band shapes give a reasonable approximation to the true absorption profile.

Ground state remission (reflectance) spectra of the TB-sensitized sepharose beads were measured at the Department of Chemistry, Loughborough University of Technology.

Monomerization of $AlPcS_2$ in solution following dilution of concentrated stock appeared to be enhanced by the presence of the microbes.

$^1O_2$ Measurements. $^1O_2$ was monitored using the collection optics and detection system described elsewhere.[51] Cells were sensitized using 1 mL D_2O/NaCl in place of PBS for the final three washes in order to enhance the lifetime of $^1O_2$ in solution. It is not known if this was sufficient to exchange cytoplasmic H_2O. Cells were suspended in long-necked quartz cuvettes (10 $\times$ 10 mm path length, 4 mL capacity), and oxygen levels were maintained by gently bubbling the suspension with compressed air, oxygen, or argon as appropriate. During measurements the gas was permitted to flow over the surface of the suspension. Quenchers were introduced as stock solutions in D_2O/NaCl.

To assess the ability of microbes to quench *extra*cellularly generated $^1O_2$, *S. mutans* and *C. albicans* in D_2O/NaCl were added in aliquots to solutions of TB, TB-immobilized on sepharose beads (see below) and $AlPcS_2$ in the same solvent, and the effect of cell concentration on $^1O_2$ lifetime was measured. Two decays were measured at each cell concentration.

Radical Anion Spectra. The sensitizer radical anion is formed by abstraction of an electron from a range of substrates by the dye triplet state. The difference spectrum of the TB radical anion is shown in Figure 5 and is characterized by absorption at 570−580 nm (63 000 M^{-1} cm^{-1}) and 635−545 nm (80 000 M^{-1} cm^{-1}), with additional weaker bands at 960−970 nm and 320−430 nm.[52,53] Clack and Yandle estimated the radical anion extinction coefficient to be approximately twice these values, with the main band relative intensities reversed,[59] while Davila and Harriman report the extinction coefficient of both bands at 27 000 M^{-1} cm^{-1}).[55]

Decays were fitted to an exponential growth and decay function after correction for emission which was not quenchable by argon purging.

Diffuse Reflectance Laser Flash Photolysis (DRLFP). DRLFP was performed as described elsewhere.[51] Cells were suspended in long-necked glass cuvettes (5 mm path length, 20 mm diameter). *C. albicans* and *E. coli* suspensions were rapidly deoxygenated by the metabolism of the cells. *P. gingivalis* and *S. mutans* suspensions were deoxygenated by bubbling with argon gas. After initial purging, oxygen was excluded in all cases by flowing argon over the surface of the sample. In some cases it was not possible to bubble the suspension directly, and a flow of argon over the sample surface proved equally effective if longer equilibration times were allowed. Suspensions were reoxygenated by bubbling with air or oxygen. Qualitative viability studies showed that a substantial proportion of *C. albicans* and *E. coli* remained viable after measurements, despite receiving lethal light doses. This was attributed to the exclusion of oxygen for most of the measurements. No attempt was made to assess membrane integrity after flash photolysis.

To avoid bleaching contributions to the DRLFP signals, suspensions were mixed by gentle agitation between each measurement. Decays were collected typically as the average of 4−8 shots (126 maximum) at 1−2 Hz.

Materials. Constant ionic strength phosphate buffered saline (PBS) was baffered to pH 7.2 $\pm$ 0.1 unless otherwise stated. Singly distilled or distilled and deionized water was used throughout.

For dispersion of *P. gingivalis*, a 70 mM solution of sodium dodecyl sulfate (SDS, Sigma) in D_2O was used.

Stock solutions of NaN_3 (Sigma, 0.3 M) and D-mannitol (Sigma 1 mol kg^{-1}) in appropriate solvents were used as $^1O_2$ and radical quenchers, respectively. Final concentrations of quencher for complete quenching were 10−20 mM.

Microbes. *Streptococcus mutans* NCTC 10449 (Gram-positive bacterium), *Escherichia coli* AB1157, *Porphyromonas gingivalis* W50 (Gram-negative bacterium), and *Candida albicans* 3019a (yeast) were the gift of Professor Mike Wilson, Eastman Dental Institute, London, and were maintained by weekly or twice weekly transfer on Wilkins Chalgren (WC) blood agar plates incubated at 37 °C. Anaerobic atmospheres were created for *S. mutans* and *P. gingivalis* using Oxoid Anaerobic Systems BR38 in gas jars.

Starter cultures of *S. mutans*, *E. coli*, and *C. albicans* were prepared by inoculating 10 mL of sterile tryptone soya broth (TSB−Oxoid, Unipath Ltd., Basingstoke, England) with single colonies taken from stock plates and incubating for 16 h. To produce experimental cultures, 0.5 mL of the starter culture was used to inoculate a further 10 mL of TSB which was then incubated without shaking at 37 °C until the culture reached the mid-log phase of growth (verified by measuring the optical density of 1 mL of culture at 540 nm).

Experimental cultures of *P. gingivalis* were prepared by suspending a generous loopful of cells in 1 mL of sterile Bacteroides Medium (BM) broth (10 g of tryptone soya, 10 g of proteose peptone, 5 g of glucose, 5 g of NaCl, 5 g of yeast extract, and 0.75 g of cysteine-HCl in 1 L adjusted to pH 7.4). This was transferred to 20 mL prereduced BM broth supplemented immediately prior to inoculation with 5 μg mL^{-1} hemin and 0.5 μg mL^{-1} Vitamin K and incubated anaerobically to the stationary growth phase.

Cells were harvested by centrifugation at 2 300 g (1 000 g for *C. albicans*) for 5 min at 4 °C. Cell numbers were determined by 4−6-fold serial dilution of experimental cultures in TSB. 20 μL aliquots of each dilution were plated onto WC blood agar and incubated for 24 h. The number of colonies was then counted, yielding the number of *colony forming units* (cfu's) (rather than actual cell numbers) in the original culture. Growth curves were determined by removing 200 μL aliquots from the growing culture at intervals and measuring the apparent optical density at 540 nm (OD_{540}) using a Labsystems Uniscan I instrument referenced against sterile TSB.

Sepharose Beads. 1.2 g of cyanogen bromide activated sepharose 4B (Sigma) (4% agarose as a lyophilised powder stabilized with lactose and dextran) was sprinkled onto 40 mL of 1 mM HCl in a sintered glass funnel at room temperature, stirred gently with a spatula, and allowed to swell for 15 min. The gel was flushed under gentle suction with 200−300 mL 1 mM HCl, ensuring that the gel was not permitted to dry, followed by 40 mL of PBS at 4 °C. The swollen gel, now at 4 °C, was suspended in 4 mL of cold 35 μg mL^{-1} TB in PBS, and incubated overnight with gentle rolling agitation at 4 °C.

The suspension was allowed to settle and a sample of supernatant removed for spectrometric determination of binding. After filtering the suspension by gentle suction, the gel was washed with 20 mL of PBS. The remaining cyanogen bromide activated groups were blocked by incubating with 1 M ethanolamine (adjusted to pH 8.0 with HCl) for 2 h at room temperature with gentle rolling agitation. The gel was again filtered under gentle suction in a sintered glass funnel and washed with four alternating cycles of 0.1 M sodium acetate buffer, pH 4 containing 0.5 M NaCl, standing for 10 min in 40 mL of each wash solution before suction was applied. A final wash of 40 mL PBS gave 4 mL of beads containing 5.5 ± 0.3 μg mL^{-1} TB. The gel was stored in an equal volume of PBS at 4 °C.

For $^1O_2$ experiments, H_2O was exchanged with D_2O by washing the gel six times with D_2O containing 0.85% w/w oven dried NaCl. The gel was allowed to stand in the D_2O/NaCl overnight in three of the washes.

Results and Discussion

Sensitizer Uptake. Figure 5 shows corrected absorption spectra for cell bound $AlPcS_2$ in whole cells and also in cells which have had their cell walls enzymatically removed (spheroplasts). $AlPcS_2$ is taken up strongly by *S. mutans* (30−60% of the sensitizer at 105 μg/10^{10} cfu was taken up by the cells). Spheroplasts of *C. albicans* and *E. coli* also demonstrate significant uptake of $AlPcS_2$, despite negligible uptake by the intact cells. This demonstrates that the main barrier to sensitizer uptake is the cell wall rather than the cytoplasmic membrane. A number of authors have found that when the integrity of Gram-negative cell walls is compromised, sensitizer uptake is enhanced and photoinactivation can be achieved in microbes which were not susceptible in their intact state.[31,32]

The most striking feature of the cellular absorption spectra is high levels of $AlPcS_2$ aggregation as evidenced by strong absorption at 590 and 780 nm which swamps the monomer Q-band at 673 nm. This is not surprising since intracellular concentrations exceed 1 mM (for 1.2×10^{10} cfu mL^{-1} *S. mutans* accumulating 33 μg mL^{-1} $AlPcS_2$ and assuming 1 cfu ≡ 5 cells, each of 0.75 μm diameter). Paardekooper et al. found that AlPc gradually monomerizes in the yeast *Kluyveromyces marxianus* but estimated that no more than 5% of the AlPc taken up became monomeric.[45] Since aggregated phthalocyanines are thought to be photochemically inactive, most of the sensitizer appears wasted.

Unlike many porphyrins, the wavelength of the monomer absorption maximum is relatively insensitive to incorporation into cells.

TB was taken up by *S. mutans*, and also by *P. gingivalis*. A typical cellular absorption spectrum is shown in Figure 3. A slight red shift is observed in the monomer absorption maximum on binding to cells. Cellular concentrations were 2−3 times higher than for $AlPcS_2$ (up to 90% uptake was achieved) and since 87% of the sensitizer localizes in the outer membranes in *P. gingivalis*, local concentrations may be even higher. A very small amount of TB is taken up by *C. albicans*, but the location is not known.[33] Surprisingly, the level of aggregation appeared to be lower than that for $AlPcS_2$. The ground state diffuse reflectance spectrum of TB-sensitized sepharose beads revealed a higher level of aggregation than in sensitized cells (see Figure 3).

Sensitizer charge is likely to play a significant role in the uptake mechanism. Gram-negative cell walls acquire a negative charge due to high lipopolysaccharide levels. Strong uptake of cationic TB and negligible uptake of anionic $AlPcS_2$ is therefore not surprising. It has recently been demonstrated that a cationic Zn phthalocyanine is taken up by Gram-negative bacteria.[57] More surprising here is the lack of uptake of either sensitizer by *C. albicans*. It may be proposed that the cell wall of *C. albicans* is extremely nonpolar so that charged sensitizers are excluded. Neutral sensitizer on the other hand is taken up by some yeasts.[45]

Simple uptake differences cannot wholly explain the different photosensitivity of Gram-positive, Gram-negative, and yeast

cells, since $AlPcS_2$ can inactivate *P. gingivalis* despite not being taken up by this organism, TB can inactivate *S. mutans* when immobilized on sepharose beads and a critical role has been observed for extra cellular haematoporphyrin in the photoinactivation of *C. albicans*.[58] Photochemical differences must also be involved, as discussed below.

Interaction of Solution Phase O_2 ($^1\Delta_g$) with Microbial Cells. In these experiments, TB was coupled to cyanogen bromide activated sepharose beads. The gel excludes molecules of mass greater than 20×10^6, and thus cells cannot penetrate the beads, which can however produce $^1O_2$ which escapes into the solvent, where it may interact with cells.

Figure 6 shows the 1270 nm luminescence observed from the beads in the presence and absence of oxygen. The residual decay in the argon-purged signal is due to the tail of the detector response to scattered laser light and TB fluorescence. No signal was observed from the same concentration of unsensitized beads. The signal was attributed to $^10_2$ on the basis of the observed wavelength, and its disappearance when the sample was purged with argon and reappearance when the sample was purged with air, as well as its decay kinetics.

After subtraction of the argon-purged signal, fitting an exponential growth and decay model to the signals yielded a decay time of 55 ± 5 μs, in good agreement with the lifetime of $^1O_2$ in D_2O measured in this work ($\tau_\Delta = 67 \pm 2$ μs, sensitized by TB) and in the literature ($\tau_\Delta = 52-70$ μs.[59] The luminescence rise time, equivalent to the TB triplet lifetime, was found to be 5.0 ± 1.3 μs, compared with a value of 2.6 ± 0.5 μs for TB-sensitized $^1O_2$ in D_2O/NaCl. This corresponds to a 50% reduction in the rate constant for quenching of TB triplets by oxygen, k'_{ox}, which is probably due to reduced diffusion rates in the beads. Such a reduction is consistent with reductions in k'_{ox} of an order of magnitude measured in some cell systems.[20,21,60,61] It proved impossible to measure TB triplet states directly by LFP or DRLFP under these conditions.

TB bound to sepharose beads is clearly able to sensitize the formation of $^1O_2$. However, since microbes cannot penetrate the beads, it must be established that $^1O_2$ can escape from the beads into the buffer in order to implicate $^1O_2$ as the active species in D_2O. The diffusion length, δ, (the distance $^1O_2$ will diffuse in a lifetime), is 2.5 μm.[18] Since cells cannot penetrate the bead, only cells within δ of the bead will come into contact with $^1O_2$. Similarly, only TB molecules bound within δ of the surface of the beads will release $^1O_2$ to a volume of solution to which the cells have access. Any quenching of $^1O_2$ by the beads will reduce the amount $^1O_2$ which escapes by reducing the value of δ in the beads.

The available evidence suggests that $^1O_2$ is not quenched by the beads. The observed $^1O_2$ kinetics were typical of $^1O_2$ in D_2O and were well described by a single first-order decay. This implies that the $^1O_2$ observed in present is only one environment, dominated by D_2O. Such a result would arise in the absence of quenching or if the beads quenched $^1O_2$ so effectively that its lifetime in the beads could not be resolved, and only $^1O_2$ escaping into the buffer would be detected. The distribution of binding sites within the beads may reasonably be assumed to be uniform, giving a maximum of 30% of the TB within δ of the bead surface. In the event of rapid quenching of $^1O_2$ by the bead, considerably less than 30% of the generated $^1O_2$ would be observed. Without correcting for higher levels of aggregation or scattering of the pump laser pulse which will both reduce the $^1O_2$ signal from the beads, the observed $^1O_2$ signal from the beads was 40% of that expected for the same concentration of TB in pure solution. It may be concluded that the beads do not appreciably quench $^1O_2$ and that the interior of the beads is dominated by the D_2O solvent. Such a result is to be expected from the bead structure.

Based on the fraction of TB within δ of the surface over the range of bead sizes, it may be calculated that 9−30% of the detected $^1O_2$ is available to cells in D_2O solution (3−11% in water where $\delta = 0.78$ μm). This correlates with a lower observed cell kill of *S. sanguis* when TB is attached to the beads compared with the same concentration free in solution, but does not explain the almost complete absence of killing of *P. gingivalis* or *C. albicans*. This latter must be explained by the inhibition of a type I or other unknown photodynamic mechanism when TB is bound to the beads.

In mechanistic terms, the inability of the beads to sensitize killing of *C. albicans* and *P. gingivalis* is explicable on the basis that $^1O_2$ alone is not sufficient to kill these organisms: a type I electron transfer process is probably required and this requires contact between sensitizer and cell. On the other hand, $^1O_2$ alone seems to be sufficient to inactivate *S. sanguis* and it is not necessary that the sensitizer be bound to the cell. This conclusion is consistent with the observation that $^1O_2$ generated *extra*cellularly using a separated surface-sensitizer system to eliminate type I processes readily deactivated *Streptococcus faecium* (Gram-positive) but only deactivated *E. coli* (Gram-negative) when the membrane had been artificially permeabilised.[62]

$^1O_2$ Emission from Sensitized *P. gingivalis* and Its Outer Membrane. 90% of the TB taken up by *P. gingivalis* is localized in the outer membrane. Isolated outer membrane fractions were shown to generate $^1O_2$ when sensitized with TB and suspended in D_2O. During D_2O exchange of the membrane preparation it was found that the isolated membrane comprised two components, one more dense and one less dense than D_2O. Measurements were made on the more dense fraction. The signal could be quenched by purging the suspension with argon and exhibited decay times typical of the D_2O solvent. Rise times could not be resolved.

Following this success, the study was extended to sensitized intact cells. Figure 7 illustrates a typical luminescence signal observed from a suspension of intact *P. gingivalis* cells sensitized with TB. The observed signal was assigned to $^1O_2$ on the following grounds: the fitted decay time ($\tau_\Delta = 58 \pm 2$ μs, obtained from global analysis of two sets of six decays, each set comprising two measurements on each of three different samples was typical of $^1O_2$ in D_2O; the signal was quenched by the addition of NaN_3 and methionine, though both may quench TB triplet states as well as $^1O_2$; and the signal disappeared when the sample was argon bubbled and reappeared when the sample was bubbled with air for 5 min.

Quenching of $^1O_2$ within *P. gingivalis*. The observed lifetime suggests that the luminescence is due to diffusion of $^1O_2$ generated in the *P. gingivalis* outer membrane into the D_2O buffer. In some experiments (Table 2) it was possible to resolve the rise time of $^1O_2$ signal which is expected to be the triplet lifetime. The measured rise time of 2.1−4.2 μs is comparable to the triplet lifetime measured in aerated solution and slightly longer than the rise time of TB-sensitized $^1O_2$ in D_2O (See Figure 8), suggesting that the rate constant for quenching of the TB triplet by oxygen was slightly reduced. This may be compared with results in other cell lines where this rate constant has been observed to decrease by an order of magnitude.[20,21,60,61] Oxygen diffusion rates are 2−5 times slower in cells than in

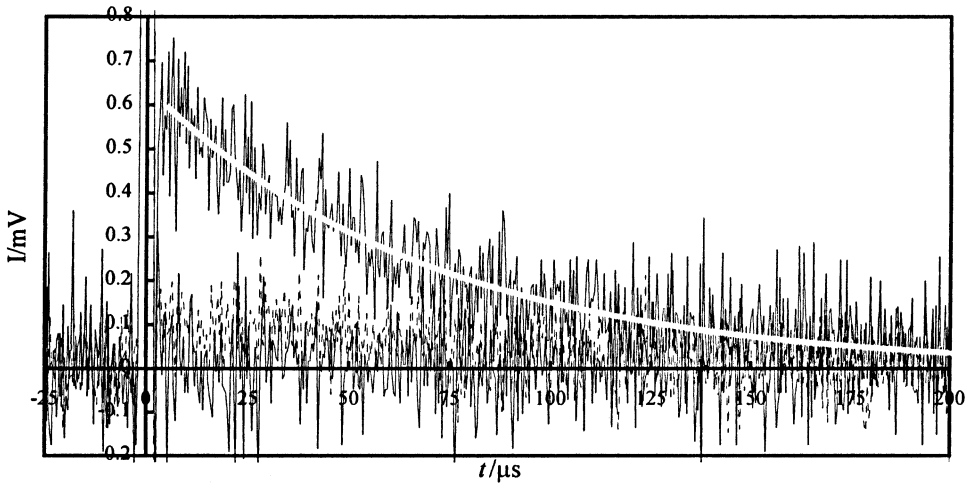

Figure 7. Time-resolved near-IR luminescence at 1 270 nm observed from a suspension of *P. gingivalis* (2.2×10^9 cfu mL^{-1}) sensitized with 26 μg mL^{-1} TB (concentration of cell-bound TB in sample is 7.4 μg mL^{-1} in D_2O/NaCl). The single-exponential fit of the $^1O_2$ decay has parameters $A = 0.64$ mV, $\tau = 69.1$ μs, $\chi^2 = 1.35$. A rise time could not be resolved. Also shown are the $^1O_2$ signal with 10 mM NaN_3 added (solid line) and of the supernatant in control cell (dashed line). The decays are the average of 128 shots at 635 nm, 0.48 mJ pulse^{-1}.

TABLE 2: Fitted Parameters for the Laser Power Dependence of $^1O_2$ Emission from *P. gingivalis*

(a) Statistics for the Global Analysis Illustrated in Figure 8

τ_1/μs	4.1	power/mJ	0.47	0.44	0.33	0.30	0.21	0.16	0.13
τ_2/μs	56.8	A	0.51	0.55	0.43	0.41	0.28	0.24	0.16
χ_g^2	0.97	χ^2	0.91	0.85	1.01	0.84	0.81	1.27	1.23

(b) Fit Parameters for the Laser Power Dependence of $^1O_2$ Emission from TB-Sensitized *P. gingivalis* and Comparison of Expected and Actual Emission Intensity

	2.2×10^9 cfu mL^{-1}		D_2O/NaCl
[TB]/μg mL^{-1}	7.4	3.7	2.44
τ_{rise}/μs[a]	2.1 ± 1.0	4.2 ± 1.0	1.8 ± 0.5
τ_{decay}/μs[a]	59 ± 3	57 ± 8	68 ± 1
χ_g^2		0.97	
intercept[b]	0.024 ± 0.024	0.008 ± 0.025	-0.03 ± 0.16
gradient/mJ^{-1} [b]	1.8 ± 0.1	1.3 ± 0.1	9.2 ± 0.7
relative gradient[c]			
no scattering	0.064	0.093	1
scattering	0.159	0.232	1

[a] Errors are standard deviation of independent fits. [b] Errors are standard deviations of the fits. [c] Corrected for concentration differences. The signal intensity in solution was shown to be linear in sensitizer concentration. Scattering was assumed to reduce the observed signal by 60% (see text). The relative gradient is the proportion of the expected $^1O_2$ luminescence which is actually observed.

buffer,[28,63,64] and so the absence of a reduction in the quenching rate constant in *P. gingivalis* reflects the proximity of the bulk of the sensitizer to the cell surface.

The luminescence observed in Figure 7 is due to $^1O_2$ which has escaped from the cells into the D_2O solvent. The proportion of $^1O_2$ quenched by the cell was estimated using a modification of the method of Baker and Kanofsky.[28,29] This relies on upon determining the luminescence intensity observed from sensitized cells as a fraction of the intensity expected from the same concentration of sensitizer free in solution. Emission intensity at a given concentration of TB in the cells was determined accurately by measuring the laser power dependence of the signal amplitude.

Laser power at 635 nm was varied over the range 0−0.55 mJ pulse^{-1}. No more than three measurements were made on any one sample, and in most cases only two were made. Seven different powers were used for each sample. Amplitudes were obtained by global analysis of the decays in each concentration set, assuming the signal grow in and decay rates were power independent and allowing the amplitude to vary independently for each decay. Fits were over the range 5−200 μs. The quenched signal showed no trace of artifacts due to tailing of the detector response, and so the background was not subtracted. The gradients of the power curves were obtained by linear regression with simple weighting.

A typical decay is shown in Figure 8, together with a complete set of residuals from the global analysis of the 3.7 μg mL^{-1} data.

The kinetic model used to fit these data was as follows, with reference to the processes outlined in Figure 9. The sensitizer triplet is typically formed in a few nanoseconds and decays on a microsecond time scale even in oxygen saturated environments. The triplet formation kinetics may therefore be ignored and it may be assumed that the laser pulse instantaneously generates an initial triplet concentration $[T]_0$. The intensity of $^1O_2$ luminescence at 1270 nm is proportional to its concentration, which is given by

$$\frac{d[T]}{dt} = -k_T[T] - k_{QT}[QT][T] - k_{OX}[O_2][T] = -k'_T[T] \quad (1)$$

$$\frac{d[^1O_2]}{dt} = S_\Delta k_{OX}[O_2][T] - k_{\Delta r}[^1O_2] - k_{\Delta nr}[^1O_2] - k_{Q\Delta}[Q_\Delta][^1O_2] = S_\Delta k_{OX}[T] - k_\Delta[^1O_2] \quad (2)$$

where k_T is the intersystem crossing rate constant for triplet deactivation, k_{QT} is the rate constant for quenching of the triplet by non-oxygen, Q_T, k_{OX} is the rate constant for quenching of the triplet state by oxygen, $k_{\Delta r}$ and $k_{\Delta nr}$ are the radiative and nonradiative rate constants for solvent deactivation of $^1O_2$, and $k_{Q\Delta}$ is the quenching rate constant for $^1O_2$ deactivation by quenchers Q_Δ. $k_{Q\Delta}$ is the sum of the reactive ($k_{Q\Delta r}$) and physical ($k_{Q\Delta p}$) quenching rate constants. S_Δ is the fraction of quenchings of the triplet by oxygen which lead to $^1O_2$ formation. Often $S_\Delta = 1$; however, it will be lower if charge transfer or enhanced intersystem crossing quenching of the triplet is significant, if the triplet lifetime is small, or if the (nonluminescent) encounter complex is long lived and does not fully dissociate.[61] The

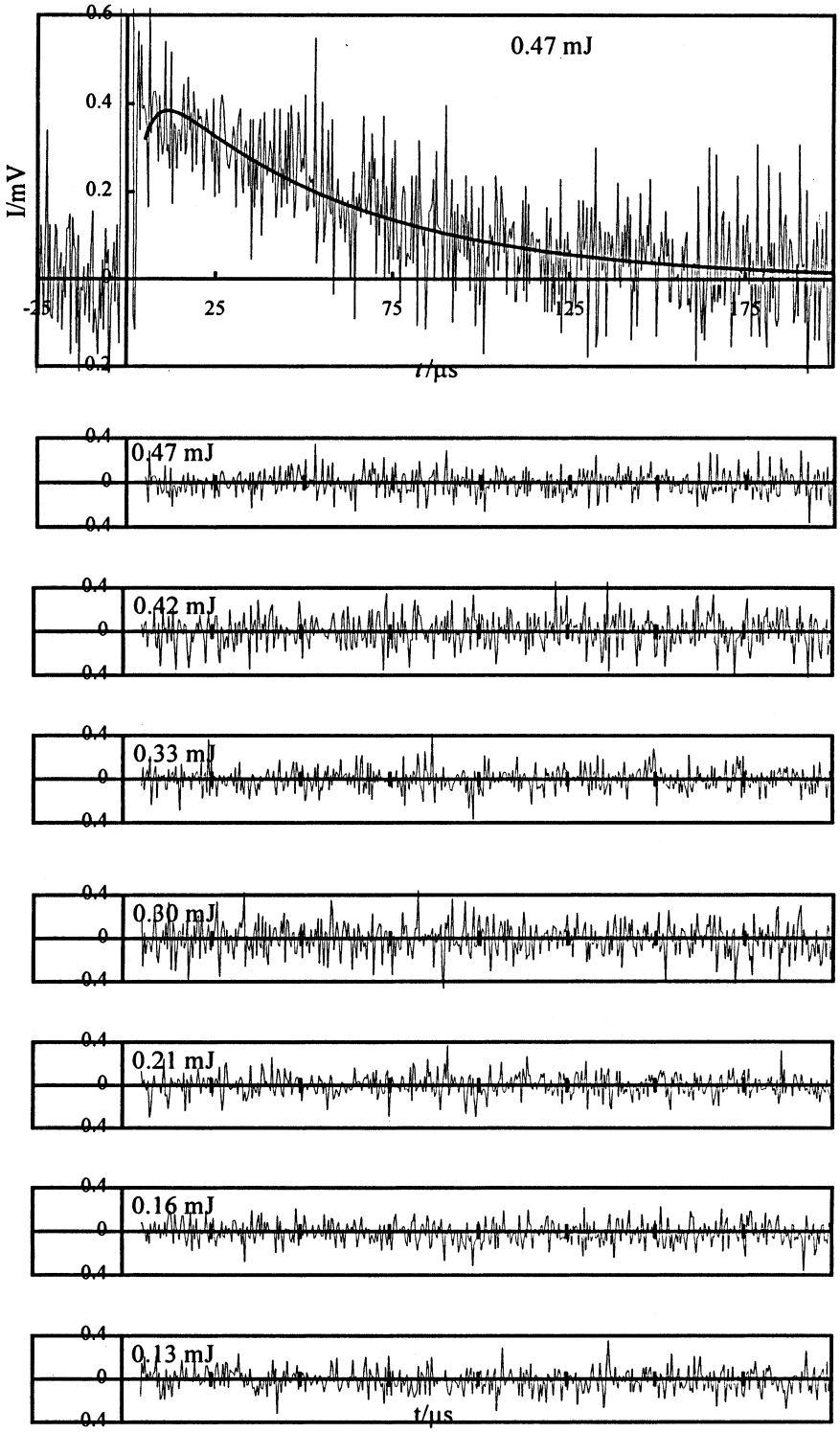

Figure 8. Typical $^1O_2$ luminescence decay and complete residuals set resulting from global analysis of the power dependence of $^1O_2$ emission *P. gingivalis* (2.2×10^9 cfu mL^{-1}, 3.7 μg mL^{-1} TB). Labels indicate the laser power used.

simplifications are made by assuming that $[Q_T]$, $[Q_\Delta]$, and $[O_2]$ are constant, giving

$$k'_T = k_T + k_{QT}[Q_T] + k_{OX}[O_2]$$

$$k'_{OX} = k_{OX}[O_2]$$

$$k_\Delta = k_\Delta + k_{\Delta nr} + k_{Q\Delta}[Q_\Delta]$$

The quantum yield of $^1O_2$ formation, Φ_Δ, is given by:

$$\Phi_\Delta = \Phi_T \frac{S_\Delta k_{OX}[O_2]}{k_{OX}[O_2] + k_T + k_{QT}[Q_T]} \quad (3)$$

In the absence of quenchers, $k_{OX}[O_2] \gg k_T$ (usually) and so $\Phi_\Delta = S_\Delta \Phi_T$. Any competitive triplet quenching process will reduce Φ_Δ and thus in vitro measurements of Φ_Δ are not indicative of in vivo Φ_Δ unless it can be shown that $k_{QT}[Q_T] = 0$ in vivo.

The solution of eq 1 is

$$[T] = [T]_0 \exp(-k'_T \tau) \quad (4)$$

which may be substituted into eq 3.3 to give:

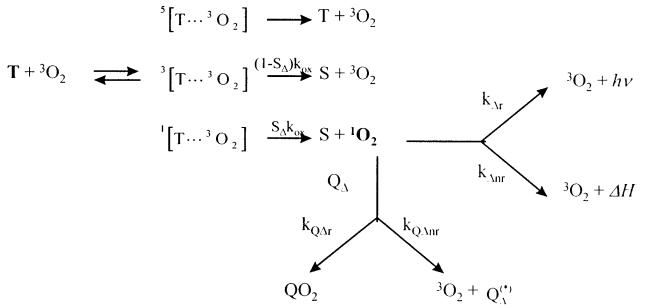

Figure 9. Processes involved in the formation and decay of $^1O_2$. T and S are the sensitizer triplet and singlet, respectively, and Q_Δ is a general quencher.

$$\frac{d[^1O_2]}{dt} + k_\Delta[^1O_2] = S_\Delta k_{OX}[T]_0 \exp(-k'_T t) \qquad (5)$$

This may be solved in a number of ways. The method of integration factors which will be applied here uses the integration factor $\exp(k_\Delta t)$. Equation 5 becomes:

$$\frac{d}{dt}\{[^1O_2]\exp(k_\Delta t)\} = S_\Delta k_{OX}[T]_0 \exp(-k'_T t)\exp(k_\Delta t) \qquad (6)$$

which can now be integrated noting the boundary condition $[^1O_2] = 0$ at $t = 0$, to give the desired expression:

$$[^1O_2] = \frac{S_\Delta k'_{OX}[T]_0}{k_\Delta - k'_T}[\exp(-k'_T t) - \exp(-k_\Delta t)] \qquad (7)$$

In the absence of triplet quenchers other than oxygen, $k'_{OX} \approx k'_T$ since $k_{OX}[0_2] \gg k_T$. Thus, $^1O_2$ luminescence is expected to exhibit an exponential grow-in and decay, with both exponents having a common preexponential factor. Whether the grow-in or decay rate constant correlates with the triplet or $^1O_2$ lifetime depends on the relative magnitude of the two terms.

The fit parameters for eq 7 to the data are listed in Table 2a and the power dependence of the $^1O_2$ emission is plotted in Figure 10. The gradients of the plots in Figure 10 are proportional to the luminescence yield from the sample. When corrected for the TB concentration of each sample, the relative gradient is equal to the fraction of expected $^1O_2$ emission which is actually observed. The intensity of $^1O_2$ luminescence of TB in D_2O/NaCl was linear with TB concentration over the range used.

Table 2 shows that between 6.4% and 23.2% of the $^1O_2$ emission expected from *P. gingivalis* is observed. The assumption that the remainder is quenched by the cell presupposes that the yield of $^1O_2$ within the cell is the same as for the same concentration external to the cell. For TB this may be valid since cell absorption spectra suggested that levels of aggregation were similar to those observed in solution but does not allow for a contribution to TB triplet deactivation by type I quenching.

These results may be compared with the 1.1 ± 0.2% of expected $^1O_2$ emission observed from *L1210 leukaemia* cells labeled with eosin[28] or Photofrin II.[39] Such a comparison implies that quenching of $^1O_2$ in L1210 cells is at least 5.8 times more effective than in *P. gingivalis*. Such a result could be attributed to the sensitizers being located deeper in the L1210 cells than in *P. gingivalis* with the result that $^1O_2$ must diffuse further to escape from the cell. However, the eosin derivative used is retained selectively in cell membranes[65] and mathematical modeling suggested that it located in the outer membrane.[28] In the previous studies, the expected $^1O_2$ signal was measured using

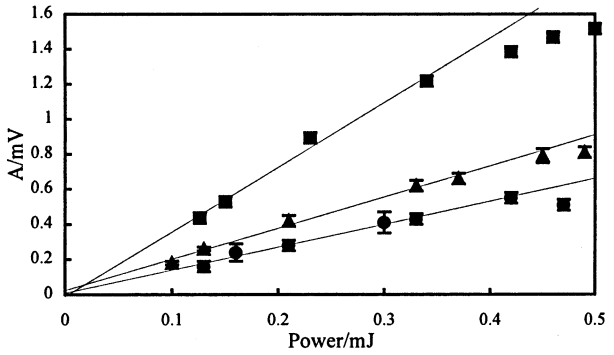

Figure 10. Laser power dependence of $^1O_2$ luminescence amplitude in 2.2×10^9 cfu mL^{-1} *P. gingivalis* 7.4 μg mL^{-1} (▲) and 3.7 μg mL^{-1} (●) TB in cells, and 2.44 μg mL^{-1} TB (■) in D_2O/NaCI. Error bars are the standard deviations of individual biexpotential fits to each of the decays. Typical residuals and fit parameters are shown in Figure 8.

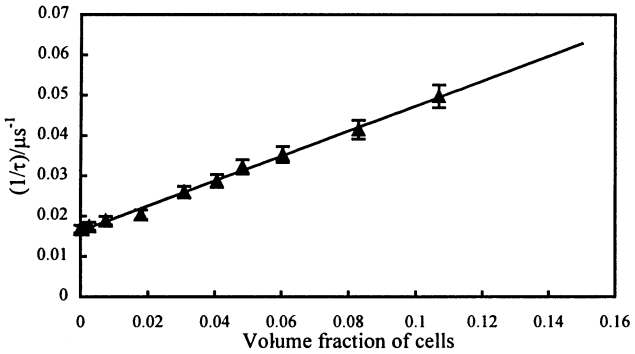

Figure 11. Stern−Volmer plot for the quenching of $^1O_2$ by *P. gingivalis* dispersed in 70 mM SDS/D_2O/NaCl. $^1O_2$ was sensitized using 4.2 μg mL^{-1} $AlPcS_2$ and 0.67 mJ $pulse^{-1}$ at 670 nm.

detergent dispersed dye, whereas the present work did *not* use detergent. Numerical modeling of *erythrocyte ghosts* (red blood cell membranes) suggested that 11% of $^1O_2$ generated within the ghosts would escape, although the model in that case allowed $^1O_2$ to escape in both directions, rather than simply outward.[27] Oelckers et al. found that the $^1O_2$ signal from a bacteriopheophorbide derivative in *erythroycte ghosts* was 5% of that which would be expected to ethanol solution.[66] The conclusion that *P. gingivalis* quenches $^1O_2$ less effectively than L1210 cells suggests that the lifetime of $^1O_2$ within *P. gingivalis* might be considerably longer than in L1210 cells.

Lifetime of $^1O_2$ within *P. gingivalis*. The lifetime of $^1O_2$ within *P. gingivalis* was estimated using the method described by Baker and Kanofsky.[20,74] Unsensitized *P. gingivalis* (6×10^{10} cfu) was dispersed in 4 mL of 70 mM SDS/D_2O/NaCl to produce a transparent straw yellow suspension. The lifetime of $^1O_2$ generated by 4.2 μg mL^{-1} $AlPcS_2$ in 70 mM SDS/D_2O/NaCl was measured as a function of the volume fraction of *P. gingivalis*. The resulting Stern−Volmer plot is shown in Figure 11. *P. gingivalis* cells were assumed to be 0.5×1 μm rods (based on electron microscopy).[33] As *P. gingivalis* grows in clusters of 10−50 cells in liquid culture,[33] an approximation of 1 cfu = 10 cells was made. The calculated pure cell pellet volume was then 0.5 mL, in good agreement with the observed pellet volume. Extrapolating the plot in Figure 11 to a volume fraction of 1.0 (pure cells) yields a cellular lifetime of $^1O_2$ in *P. gingivalis* of 3.1 ± 0.6 μs (the error includes an allowance for error in the estimate of cell volume).

It is clear from this that the nonaqueous material in *P. gingivalis* quenches $^1O_2$ at least an order of magnitude more

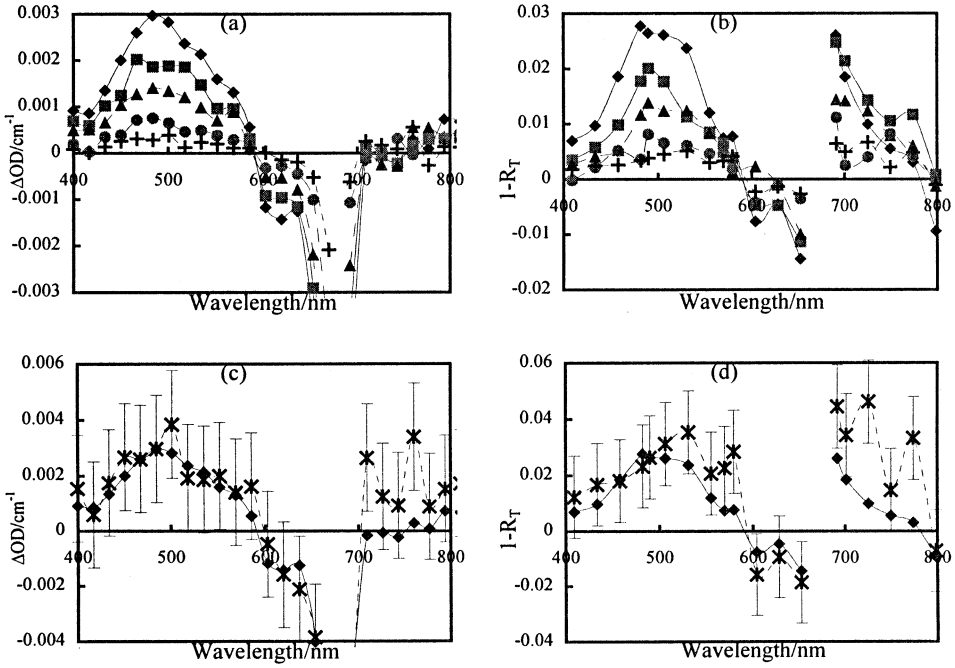

Figure 12. Time-gated transient absorption spectra for $AlPcS_2$ in deoxygenated PBS (a) in solution and (b) 35 μg mL^{-1} with 4×10^8 cfu mL^{-1} *C. albicans.* Comparison of transient spectra at 10 μs (◆) and 850 μs (×) in the decay, reveal that in solution (c) the spectrum is independent of decay time, while in the presence of *C. albicans* (d) a long-lived component is present in the region of 530−570 nm which has been assigned to the $AlPcS_2^{\bullet-}$ radical anion. In (c) and (d) spectral pairs have been normalized to the same intensity at 484 nm (the triplet maximum). Excitation at 673 nm. Decays are the average of no more than 16 shots. Each point is typically the average of 20 points (20 μs) in the measured decay. Error bars are the standard deviation of two measurements at 565 nm.

slowly than the nonaqueous material in the mammalian cell lines that have been the subject of previous studies.

Baker and Kanofsky, in an elegant series of experiments, estimated that lipids were responsible for only 2−7% of the quenching of $^1O_2$ in *RBC ghosts*[27] and less than 0.1% in L1210 cells.[28] The bulk of the quenching in both cases was attributed to proteins. Microbe cell walls have higher lipid and lower protein contents than eucaryotic cells. Lipids are known to quench $^1O_2$ with rate constants an order of magnitude lower than proteins and so this may explain the longer lifetime of $^1O_2$ in *P. gingivalis* and may explain why Gram-negative bacteria are difficult to kill.

Type I Processes. Results on cell walls above suggest something other than $^1O_2$ is required to inactivate *P. gingivalis* and *C. albicans*. A type I process involving electron transfer to or from the sensitizer triplet state is the most likely candidate, and the aim of the work presented in this section was to detect the products of type I reactions in cellular media by monitoring the transient radical spectrum of the sensitizer. The majority of the work utilized $AlPcS_2$ as a sensitizer for two reasons: it has greater photostability under the conditions of high pump and probe powers required for DRLFP, and its transient species have larger extinction coefficients and so permit greater sensitivity.

Electron transfer to or from the sensitizer triplet state contributes to the general deactivation of the sensitizer excited state, resulting in a reduction in the triplet lifetime and the formation of a sensitizer radical ion. The sensitizer radical ion has a characteristic absorption spectrum and so the decay of the triplet absorption in the presence of a type I process should be accompanied by the growth and decay of absorption due to the (transient) radical ion. However, for small quenchings of the triplet state, signals may be difficult to detect. The presence of the radical anion can be detected by normalizing spectra at different delay times to that of the triplet absorption maximum, as shown in Figure 12, and by using global analysis of the kinetic scheme below.

The rate equations for the sensitizer triplet state (T) decay and the radical ($S^\bullet$) growth and decay are

$$d[T]/dt = -(k_T + k_{QR}[Q_R])[T] \quad (8)$$

$$d[S^\bullet]/dt = k_{QR}[Q_R][T] - k_R[S^\bullet] \quad (9)$$

where k_{QR} is the rate constant for type I triplet quenching by the donor/acceptor Q_R and k_R is the rate constant for radical decay. In this context, and setting $k'_T = k_T + k_{QR}[Q_R]$, they give

$$[T] = [T]_0 \exp\{-[k'_T)t]\} \quad (10)$$

$$[S^\bullet] = \frac{k_{QR}[Q_R][T]_0}{k'_T - k_R}\{\exp[-k_R t] - \exp[-k'_T t]\} \quad (11)$$

or if $k_R \ll k_T + k_{QR}[Q]$ i.e., the radical is long-lived relative to the triplet:

$$[S^\bullet] = \frac{k_{QR}[QR][T]_0}{k'_T}\{1 - \exp[-k'_T t]\} \quad (12)$$

Let $\epsilon_{S^\bullet}$ and ϵ_T be the radical and triplet extinction coefficients, respectively, so

$$\Delta OD = \epsilon_T[T] + \epsilon_{S\bullet}[S^\bullet]$$

i.e., using eqs 10 and 11

$$\Delta OD = \frac{\{\epsilon_T(k_T - k_R) + (\epsilon_T - \epsilon_{S\bullet})k_{QR}[Q_R]\}[T]_0}{k'_T - k_R} \times \exp[-k'_T t] + \frac{\epsilon_{S\bullet}k_{QR}[Q_R][T]_0}{k'_T - k_R}\exp[-k_R t] \quad (13)$$

or in the limit of long radical lifetime:

$$\Delta OD = \frac{\{\epsilon_T k'_T - \epsilon_S \cdot k_{QR}[Q_R]\}[T]_0}{k'_T} \exp[-k'_T t] + \frac{\epsilon_S \cdot k_{QR}[Q_R][T]_0}{k'_T} \quad (14)$$

Equations 13 and 14 demonstrate that the decay in the presence of a radical can be modeled as the sum of two exponentials, one with the triplet lifetime and one with the radical lifetime. The sign and relative magnitude of the amplitudes depend in a complex way on the interplay of rate constants and extinction coefficients.

Comparing eqs 11 and 13, the amplitude of the second component of the transient decay is the product of the radical extinction coefficient and the amplitude of the radical contribution to the transient concentration. Thus the wavelength dependence of the amplitude associated with the radical ion lifetime (which will have zero amplitude at a region where the radical ion does not absorb) will give the transient radical difference absorption spectrum. A plot of the decay amplitude at $t = 0$ (i.e., the sum of the fitted amplitudes) will reveal the triplet difference absorption spectrum. The ratio of the amplitudes of the radical and triplet spectra determined in this way is

$$\frac{I_R}{I_T} = \frac{\epsilon_S \cdot [k_{QR}[Q_R]]}{\epsilon_T [k'_T - k_R]} \quad (15)$$

Since the radical quantum yield from the triplet state is given by

$$\Phi_{Rad} = \frac{k_{QR}[Q_R]}{k'_T} \quad (16)$$

It is clear that the radical yield cannot be obtained from the fitted spectrum directly, but requires a knowledge of the extinction coefficients and k_R.

This biexponential model has the disadvantage of being sensitive to signal noise. Spurious amplitudes and kinetics can arise as a result of the minimization process fitting noise, particularly where the radical yield is low and the signal/noise ratio is low, as is the case in DRLFP measurements on cell suspensions. The model is slightly less sensitive to noise if both amplitudes can be assumed to be positive and thus constrained during the fit. This will be the case where the radical ion is relatively long-lived and the yield is low.

An alternative approach, which is less sensitive to signal noise, is available if it can be assumed that the radical lifetime is long compared to the triplet lifetime and the time window being studied. In this case, the transient absorption is described by eq 14. The transient spectrum can then be modeled by a single-exponential decay with constant offset where the offset is the product of the absolute radical yield (eq 12) and the radical extinction coefficient $\epsilon_S \cdot$. In this case the wavelength dependence of the offset will reproduce the transient radical ion spectrum. As before, the initial amplitude (now the decay amplitude plus the offset) will yield the triplet spectrum. Modeling shows that analysis using this model is less sensitive to artifacts, and the offset clearly reveals the transient spectrum of $AlPcS_2^{\bullet -}$ in the presence of ascorbate, while giving a random fluctuation about the baseline in the absence of ascorbate. The ratio of the amplitudes of the spectra determined in this way is

$$\frac{I_r}{I_r} = \frac{\epsilon_S \cdot [k_{QR}[Q_R]]}{[k'_T]} = \frac{\epsilon_S \cdot}{\epsilon_T} \Phi_{rad} \quad (17)$$

and so the radical yield can be determined directly from the fitted spectrum provided the extinction coefficients are known and the assumption concerning k_R holds.

When Gaussian noise comparable to that observed experimentally was applied to simulated data, both models gave the same band contours and surprisingly the same relative amplitude for the radical band which was in good agreement with the result obtained by fitting a single exponential with offset to noise free data. The data outlined below were obtained using these methods.

Extracellular Sensitizer, $AlPcS_2$. Figure 12 compares the transient diffuse reflectance spectrum of $AlPcS_2$ recorded in the presence of *C. albicans* with the transient transmission spectrum recorded in PBS. No signal was obtained from a suspension of cells without $AlPcS_2$. The dominant feature of the transient absorption was attributed to the $AlPcS_2$ triplet on the basis of its peak absorption at 480−500 nm, in good agreement with the solution phase result, and by the fact that it could be quenched by purging the suspension with oxygen and recovered by purging the suspension with argon. Oxygen quenching rate constants are estimated to be greater than 5×10^8 M^{-1} S^{-1} on the basis that the triplet lifetime became shorter than the time resolution of the DRLFP system when samples were bubbled with oxygen. As expected, this is comparable to solution phase values.

When the shape of the transient spectrum at 10 μs was compared with that at 850 μs (Figure 12c,d), the solution phase spectrum demonstrated extremely good overlap, confirming that all transient species followed the same kinetics. On the other hand, when *C. albicans* was added to the suspension, although errors in individual points are large, a definite systematic variance is clear between the early and late time spectra. The distinct shift to longer wavelengths of the late time spectrum is indicative of a *second* transient species with different kinetic behavior to the triplet and characteristic of the changes expected if triplet $AlPcS_2$ was converted to the $AlPcS_2^{\bullet -}$ radical anion. Similar results were obtained for *E. coli* and *P. gingivalis*. To test the assignment, spectra were analyzed globally as described above. The results for all three cell types are presented in Figure 13. Representative decays and typical global fit residuals are shown in Figure 14. The corresponding fit parameters are listed in Table 3.

Figure 13 reveals a relatively long-lived species with an absorption band at 550−570 nm in suspensions of *E. coli* and *C. albicans*. Absorption in this region is characteristic of the $AlPcS_2^{\bullet -}$ radical anion in solution when detected at low levels by the same techniques and consistent with published spectra of the $AlPcS_2^{\bullet -}$ anion. A lower concentration of $AlPcS_2$ was used to record the spectrum of *P. gingivalis*, hence the lower intensity and precision. The offset spectrum is suggestive but not definitive evidence for the formation of the $AlPcS_2^{\bullet -}$ radical anion in this case. When compared to the random spread of offsetsfor $AlPcS_2$ in H_2O or in *S. mutans*, the trend line through the data is suggestive of an absorption in the region of 570 nm. Further measurements at higher concentrations of cells and $AlPcS_2$ are expected to confirm the presence of the radical anion in *P. gingivalis*. Further confirmation of the assignment was sought in the case of *C. albicans* by adding 20 nM mannitol, a radical quencher, to the suspension. This appeared to remove the long-lived component of the decay at 570 nm; however, the difference was not statistically significant and insufficient data were collected to permit spectral analysis.

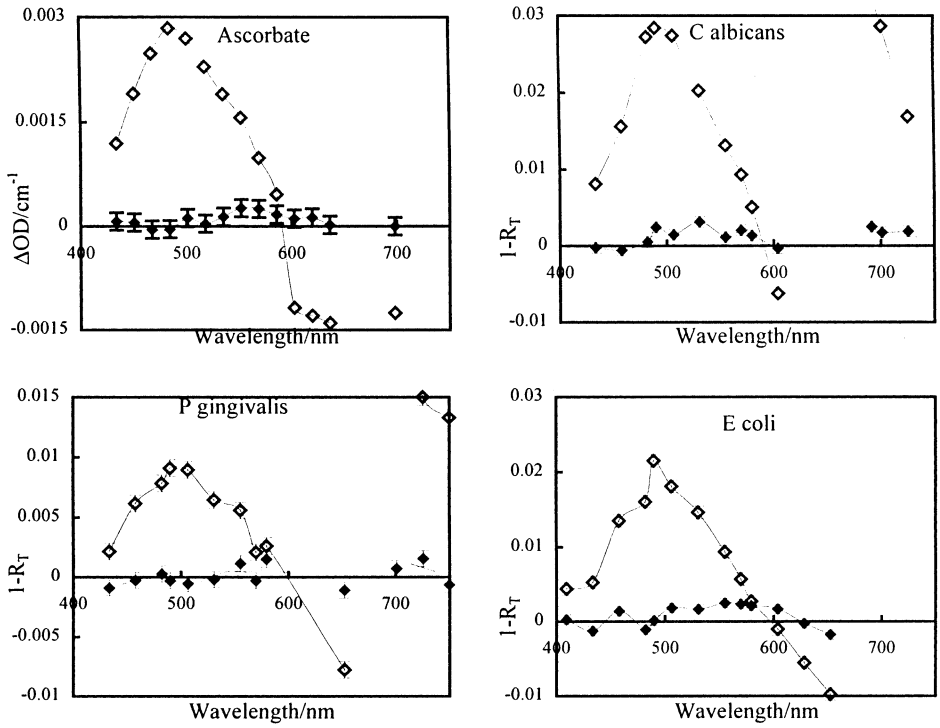

Figure 13. Wavelength dependence of triplet amplitudes (open symbols) and offsets (closed symbols) resulting from global fitting of $AlPcS_2$ transients to a single exponential with offset in the presence of 5.4×10^{-6} M ascorbate: 4×10^8 cfu mL^{-1} *C. albicans*; 6.7×10^{10} cfu mL^{-1} *P. gingivalis*; 1×10^{11} cfu mL^{-1} *E. coli*. $AlPcS_2$ concentrations were 35 μg mL^{-1} except for *P. gingivalis* (26 μg mL^{-1}). A trend line has been used for *P. gingivalis* offsets. Other lines are smoothed curves through all points. All spectra recorded in the absence of oxygen and at pH 7.1 except ascorbate (pH 6.3). Laser powers for cell suspensions were typically 3 mJ pulse^{-1} at 673 nm and decays were the average of no more than 16 shots. Errors are the average standard deviation of fit parameters by global analysis of different combinations of wavelengths. A typical decay and residuals set is shown in Figure 14. $(1 - R_T)$ is the diffuse reflectance equivalent of ΔOD.

Together the comparison of early and late time transient absorption spectra (Figure 12d) and the spectral profiles extracted by global analysis of the decays (Figure 13) lead to the conclusion that in these cell lines, in the absence of oxygen, $AlPcS_2$ is partly quenched by a type I process producing the $AlPcS_2^{\bullet-}$ radical anion in low yield. The photophysical parameters of $AlPcS_2$ in cellular environment as measured in this work are summarized in Table 4.

The radical yields listed in Table 4 were calculated from eq 17 assuming $\epsilon_{T490} = 36\,000$ M^{-1} cm^{-1} and $\epsilon_{S^\bullet\,570} = 63\,000$ M^{-1} cm^{-1}. No correction was made for the contribution of singlet depletion (which would increase the radical yield). Since the radical yield is dependent upon the concentration of quencher, the values listed in Table 4 are expected to increase with increasing cell concentration.

The triplet lifetimes reported in Table 4 were obtained as parameters of the global analysis used to identify the generate Figure 13. Decays were modeled using a single exponential with a fluctuating offset. Reported lifetimes are the average $\pm$ sample standard deviation of at least two fits to different sets of 10 transient decays chosen to include the complete spectral region covered. In general, higher yields correspond to shorter triplet lifetimes, as would be expected as the extent of quenching increases.

Extracellular Sensitizer, TB. *C. albicans* was the only organism studied which did not take up TB. Since the yeast reduces TB in the absence of oxygen, transient spectra could only be measured in aerated solution where any radical products would rapidly be reoxidized. Under these circumstances, the transient spectrum of TB was observed to have a maximum absorption between 440 and 460 nm, in agreement with the solution phase spectrum. The transient had a lifetime (determined by a global single-exponential fit to the spectrum) of approximately 9 μs. Interference from scattered laser light limited the temporal resolution of these measurements.

Intracellular Sensitizer, $AlPcS_2$. Figure 15 shows the transient absorption spectrum of $AlPcS_2$ incorporated into *S. mutans*. The photophysical properties of $AlPcS_2$ obtained from this spectrum are also listed in Table 4. No signal was observed when the supernatant was recovered by centrifugation and used to suspend the same number of unsensitized control cells, confirming that all the observed signal was due to intracellular sensitizer. Although the concentration of $AlPCS_2$ in the sample was similar to that used in the extracellular studies on *C. albicans* and *E. coli*, a much lower transient intensity was observed in *S. mutans*. This may have been due to a combination of increased sensitizer aggregation and a reduction in the effective scattering and absorption coefficient due to the need for light to now penetrate the cells in order to reach the sensitizer. Without knowing the scattering properties of the different cell types it is not possible to identify precisely the cause of the reduced intensity. The signal intensity was independent of the laser power used.

In contrast to the spectra shown in Figures 12 and 13, the excellent overlap of the early and late time transient spectra in Figure 15 suggests that a type I quenching of $AlPcS_2$ by *S. mutans* does not occur, or is at least several times less efficient than that by other organisms studies. Global analysis of the spectrum tends to confirm this: the offset component is close to zero with no clear correlation suggestive of absorption, and compares favorably with the spectrum of $AlPcS_2$ in PBS.

Intracellular Sensitizer, TB. Transient species were detected in TB-sensitized *S. mutans* and *P. gingivalis* and also in

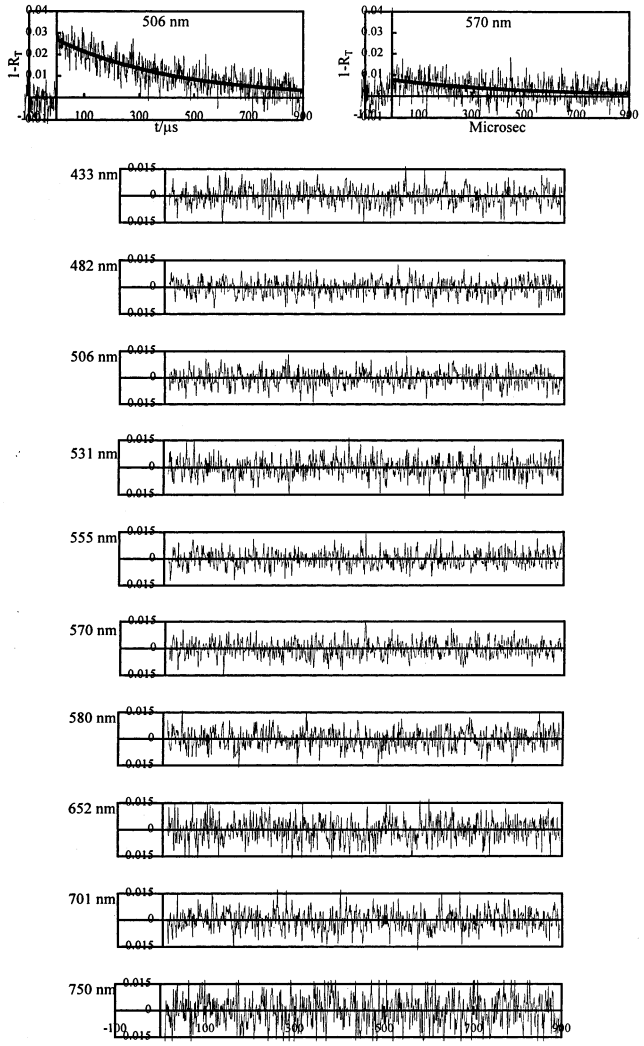

Figure 14. Typical decays from 35 μg mL^{-1} $AlPcS_2$ with 4×10^8 cfu mL^{-1} *C. albicans* in deoxygenated PBS pH 7.1 and residuals resulting from global analysis of a family of such decays using a single exponential with offset model (see text).

sensitized outer membrane fractions isolated from *P. gingavalis*. Assignment and interpretation of the results is more difficult than for $AlPcS_2$ due to the rapid bleaching of the dye, caused primarily by the Xe probe lamp and considerably lower signal intensity (due to lower transient extinction coefficients for TB cf. $AlPcS_2$).

Transient spectra recorded in TB-sensitized *P. gingivalis* and its outer membrane are shown in Figure 16. Exchange of the sample supernatant with an unsensitized control sample of the outer membrane showed that all the signal arose from membrane bound TB. Good agreement was observed between the transient reflectance spectra and the transient transmission spectrum of the monocation triplet state of TB, pH 8.9. Transients in 9.2×10^9 cfu mL^{-1} *S. mutans* containing 61 μg mL^{-1} TB had a lifetime in the absence of oxygen of 85 μs (measured over 90 μs of decay) which compares with 58 μs in PBS pH 8.5. The transient lifetime in *P. gingivalis* was in excess of 100 μs.

More rigorous analysis could be conducted on isolated *P. gingivalis* outer membrane, where a lifetime of 152 ± 9 μs was measured. An additional long-lived component (modeled as an offset) had comparable intensity to the decaying component and uniform intensity across the spectrum. This was tentatively assigned to TB photoproducts and may have been the result of nonphotodynamic photochemistry since the transient could not be quenched by saturating the suspension with oxygen.

Figure 16b shows evidence that the ground state depletion recovered more slowly than the triplet absorption and of a longer lived transient absorbance at 760−800 nm. Since the reduced form of TB is colorless, it will not contribute to the transient difference spectrum at visible wavelengths. There is a report of the monocation of the reduced form of thionine absorbing at 780 nm, and it is reasonable to assume that leuco-TB will have a similar absorption band. Formation of reduced leuco-TB from the TB triplet will deactivate the triplet state without regenerating the ground singlet state, and so ground state depletion will return to baseline levels more slowly than excited state absorption. Figure 16b therefore provides evidence that type I processes are involved in the deactivation of the TB triplet state, although a definitive conclusion is prohibited by the obviously complex nature of the processes occurring in TB sensitized systems. It is not known how rapidly, if at all, TB was reoxidized in this experiment.

TABLE 3: Global Fit Parameters for the Data Set Illustrated and Described in Figure 14[a]

τ/μs	423	λ/nm	433	482	506	531	555	570	579	652	701	750
χ_g^2	1.01	$A/10^{-3}$	8.5	27.3	26.7	17.5	12.2	7.2	3.6	−16.6	27.3	12.5
		$R/10^{-4}$	−4.5	−6.1	2.5	24.3	7.1	5.5	12.7	−1.9	10.5	21.1
		χ^2	1.26	0.91	0.75	1.34	0.96	0.85	1.09	1.10	0.98	0.99

[a] A is the amplitude of the exponential decay and R is the amplitude of the offset. The triplet spectrum is given by the wavelength dependence of $(A + R)$, the transient radical spectrum by the wavelength dependence of R.

TABLE 4: Photophysical Parameters of $AlPcS_2$ in Microbial Cell Environments[a]

system	λ_T^{max}/nm	I_T[b]	τ_T/μs	λ_{rad}^{max}/nm	Φ_{rad}[c]	[cells]/cfu mL^{-1}
PBS	485	0.0031_2	403 ± 10			
ascorbate	490	0.0029_2	403 ± 4	565	0.05 ± 0.01	(5.4×10^{-6} M)
C. albicans	495	0.0263_9	390 ± 30	525−540	0.07 ± 0.01	4×10^8
P. gingivalis	490	0.0095_9	460 ± 40	570	0.04 ± 0.03[d]	6.7×10^{10}
E. coli	490	0.021_2	300 ± 40	560	0.12 ± 0.09	1×10^{11}
S. mutans	500	0.0030_8	570 ± 150		<0.02[e]	1.2×10^{10}

[a] Measurement conditions are as in Figures 13 and 15. [b] Minimum values as discussed in the text. Φrad is dependent upon the concentration of the donor. These values are therefore specific to the cell concentration used. [c] No evidence of radical species apparent in fits. Maximum limit of yield determined from mean of fitted offsets. [d] Intensity units are ΔOD for solution measurements and % absorbance for cell measurements. Direct comparison between measurements is only possible by assuming S is the same for all cell lines. The values are reported as an indication of the signal resolution in different systems. [e] The value for *P. gingivalis* assumes a positive identification of the transient radical anion. See text for discussion of the limits of this assumption.

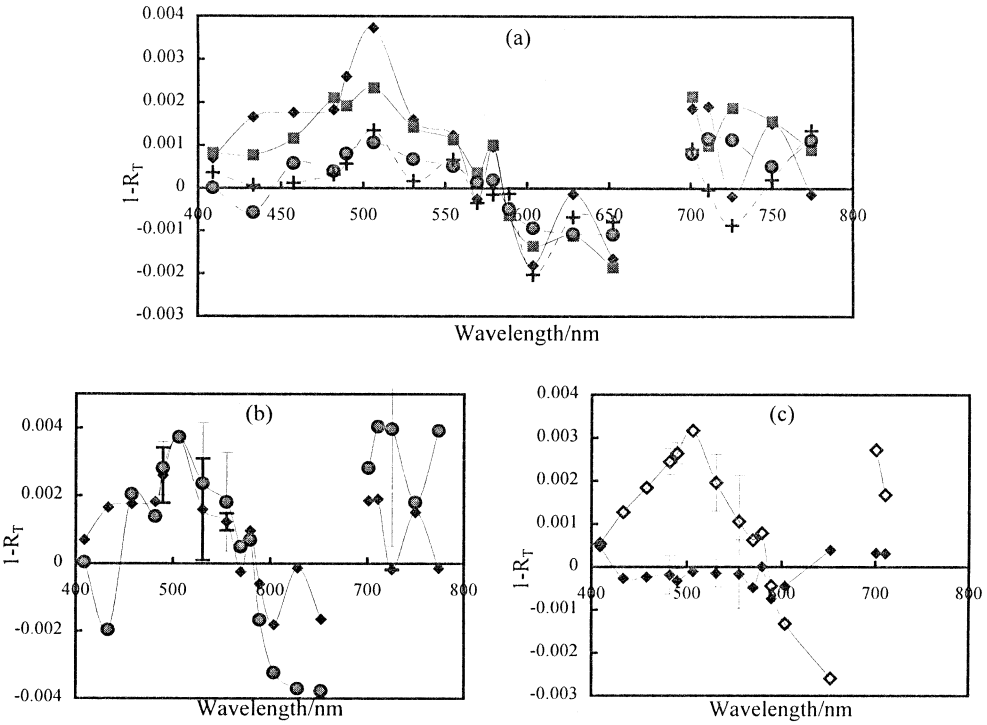

Figure 15. Transient absorption spectrum of $AlPcS_2$ in *S. mutans* 1.2×10^{10} cfu mL^{-1}, 33μg mL^{-1} $AlPcS_2$, 7.6 mJ $pulse^{-1}$ at 673 nm. (a) Data points are the average of 30 decay channels at 20, 150, 600, and 850 μs after the laser pulse. (b) Spectra at 20 μs (diamonds) and 600 μs (circles) normalized at 500 nm. (c) Triplet amplitude (open symbols) and offsets (closed symbols) from global analysis using a single-exponential and offset model. Representative error bars in (b) and (c) are the standard deviation of variations between measurements and between global analysis of different subsets of the data on the indicated wavelengths.

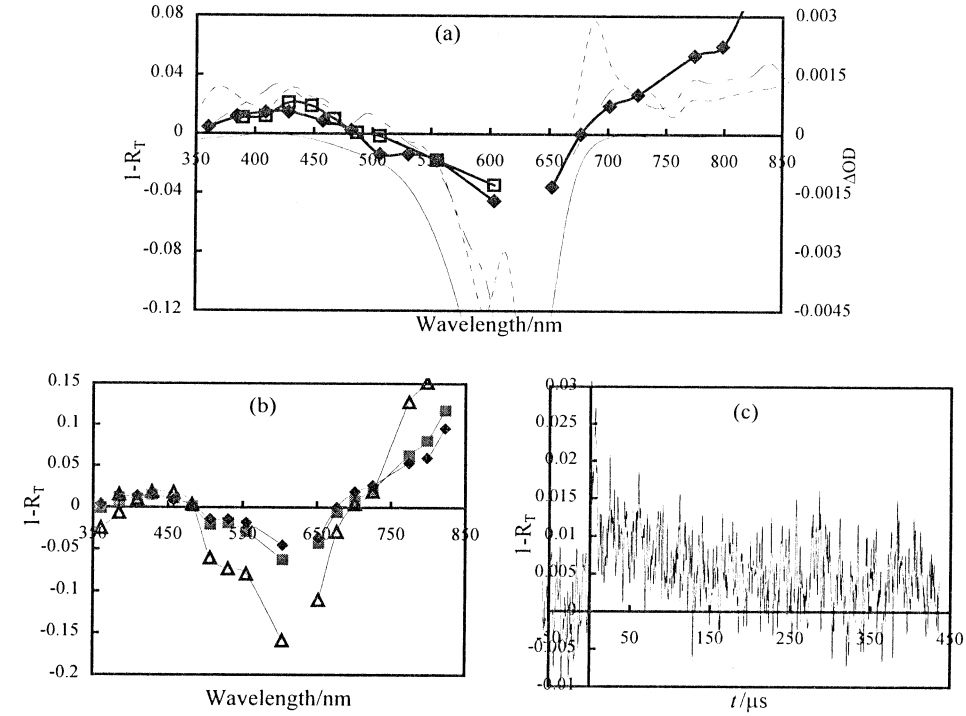

Figure 16. (a) Transient spectra recorded for TB sensitized *P. gingivalis* (3×10^{10} cfu mL^{-1}, 67 μg mL^{-1}) (open squares), and its outer membrane (diamonds). The membrane preparation was suspended in just sufficient H_2O enable it to be handled as a fluid. Also shown are the spectra of TB in PBS at Ph 4.6 ($\tau = 5$ μs) (short dashes) and pH 8.9 ($\tau = 58$ μs) (long dashes) and the ground state absorption spectrum of TB in PBS (solid line). (b) Transient spectrum of TB in *P. gingivalis* outer membrane at 400 μs (triangles) shows the slow singlet state recovery relative to the triplet decay. The spectrum is compared with the spectrum at 8 μs (diamonds) and 50 μs (squares) delays. (c) TB transient decay in *P. gingivalis* outer membrane at 428 nm.

Conclusions

It has been shown in this work that TB sensitizes the formation of $^1O_2$ even when bound to sepharose beads and this $^1O_2$ is available to cells in suspension outside the beads. $^1O_2$ alone cannot therefore be sufficient to kill *P. gingivalis* and *C. albicans*, but seems to be sufficient to kill *S. mutans*. The first direct evidence is presented here for the formation of the $AlPcS_2^{\bullet-}$ radical anion in suspensions of *C. albicans*, *E. coli*,

and probably also *P. gingivalis.* This suggests that a type I process is available to provide the additional mechanism enabling *P. gingivalis* and *C. albicans* to be inactivated. Although more difficult to measure, there is some evidence (slower ground state recovery than triplet decay) for type I processes when TB is bound to *P. gingivalis* outer membranes. Interestingly, no evidence of type I processes was found for $AlPcS_2$ in *S. mutans*, suggesting a key role for the cell wall in mediating photodynamic mechanisms. The first observation of $^1O_2$ luminescence from a suspension of bacteria is also reported. TB bound to *P. gingivalis* is capable of sensitizing the formation of $^1O_2$. 80−95% of $^1O_2$ is quenched by the bacterium and the $^1O_2$ lifetime in the cell has been estimated to be 3.1 μs. The extent of quenching and the rate of deactivation of $^1O_2$ by the cell are both an order of magnitude lower than comparable quantities measured in mammalian cell lines. This is consistent with $^1O_2$ not being sufficient to inactivate *P. gingivalis* in the absence of other mechanisms.

There is considerable indirect evidence to support a two-stage mechanism involving both type I and type II processes in a variety of microbes.

It is thus proposed here that the photoinactivation of *S. mutans* (Gram-positive bacterium) proceeds via a type II $^1O_2$ mediated process, whereas the photoinactivation of *P. gingivalis* (Gram-negative bacterium) and *C. albicans* (yeast) requires a contribution from a type I mechanism. This requires an electron donor from the cell wall constituents. Future work will seek to identify this electron donor, but it can be said that since the Gram-positive bacterium *S. mutans* is an inefficient quencher of the $AlPcS_2$ triplet state, and *S. mutans* is 60−90% peptidoglycan, PGN, this is an unlikely donor. Glucan, by contrast, may well act in this way, since *C. albicans*, glucan rich, *is* an efficient quencher of the $AlPcS_2$ triplet state. The type I process seems to initiate changes in the permeability of the cell wall of *P. gingivalis* and *C. albicans*, permitting the sensitizer and probably $^1O_2$ access to intracellular targets. The ability of TB but not $AlPcS_2$ to inactivate *C. albicans* can may be attributable to the lower reduction potential of the $AlPcS_2$ triplet compared with that of TB and the different structure of the cell walls of *C. albicans* and *P. gingivalis.* Although the reduction of $AlPcS_2$ was observed in the presence of *C. albicans*, it is suggested that the yield is insufficient to permeabilise the yeast cell wall, which is 330 nm thick (cf. 14−23 nm for *P. gingivalis*). TB's higher reduction potential would seem to result in more critical damage and hence killing of *C. albicans*. Since the species differences observed in this work appear to be mediated by the cell wall, it is possible that Gram-positive bacteria generally may be inactivated by a $^1O_2$ mechanism while Gram-negative bacteria and yeasts generally may require a contribution from type I processes. More work is needed on other organisms to justify such an extension of the present results.

Acknowledgment. We are very grateful to the Engineering and Physical Sciences Research Council, UK, for financial support. T.C.O. gratefully acknowledge the Association of Commonwealth Universities for the award of a Commonwealth Scholarship during the course of his PhD program. We thank Professor M. Wilson and his colleagues at the Eastman Dental Hospital, London, and Dr. Andrew Miller and colleagues of this Department for assistance in preparation of microbes and Professor Frank Wilkinson and colleagues for assistance with early DRLFP experiments.

References and Notes

(1) Malik, Z.; Hanania, J.; Nitzan, Y. *J. Photochem. B. Photobiol.* **1990**, *5*, 281.
(2) Wallis, C.; Melnick, J. L. *Photochem. Photobiol.* **1965**, *4*, 159.
(3) Wilson,M. *J. Appl. Bacteriol.* **1993**, *75*, 299.
(4) Saitow, F.; Nakoaka, Y. *Photochem. Photobiol.* **1996**, *63*, 868.
(5) Malik, Z.; Ladan, H.; Nitzan, Y.; Smetana, Z. *SPIE* **1994**, *2078*, 305.
(6) Tuite, E. M.; Kelly, J. M. *J. Photochem. Photobiol., B. Biol* **1993**, *21*, 103.
(7) Halliwell,B.; Gutteridge, J. M. C. *Free Radicals in Biology and Medicine*; Clarendon Press: Oxford, UK, 1989.
(8) Foote, C. S. In *Future Directions and Applications in Photodynamic Therapy*; Gomer, C. J., Ed.; SPIE Press: Washington, DC, 1990.
(9) Foote, C. S. In *Biochemical and Biophysical Aspects of Oxygen*; Coughey, W. S., Ed.; Academic Press: New York, 1979; p 603.
(10) Henderson, B. W.; Bellnier, D. A. In *Photosensitising Compounds: Their Chemistry, Biology and Chemical Use*; Ciba Foundation Symposium 146; John Wiley and Sons: New York, 1989; p 112.
(11) Ganguly, T.; Battacharjee, S. B. *Photochem. Photobiol.* **1983**, *38*, 65.
(12) Foster, T. H.; Murant, R. S.; Bryant, R. G.; Knox, R. S.; Gibson, S. L.; Hilf, R. *Radiat. Ros*. **1991**, *26*, 296.
(13) Ben-Hur, E.; Geacintov, N. E.; Studamire, B.; Kenney, M. E.; Horowitz, B. *Photochem. Photobiol.* **1995**, *61*, 190.
(14) Moan, J.; Petterson, E. O.; Christensen, T. *Brit. J. Cancer* **1979**, *39*, 398.
(15) Pardekooper, M.; De Bruijne, A. W.; Van Steveninck, J.; Van den Broek, P. J. A. *Photochem. Photobiol.* **1995**, *61*, 84.
(16) Pardekooper, M.; Van den Broek, P. J. A.; De Bruijne, A. W.; Elferink, J. G. R.; Dubbelman, T. M. A. R.; Van Steveninck, J. *Biochim Biophys Acta* **1992**, *1108*, 86.
(17) Menezes, S.; Capella, M. A. M.; Caldas, L. R. *J. Photochem. Photobiol. B: Biol.* **1990**, *5*, 505.
(18) Lissi, E. A.; Encinas, M. V.; Lemp, E.; Rubio, M. A. *Chem. Rev.* **1993**, *93*, 699.
(19) Roberts, J. E.; Atherton, S. J.; Dillon, J. *Photochem. Photobiol.* **1991**, *57*, 855.
(20) Crow, M.; Redmond, R.; Truscott, T. G. *J. Chem. Soc., Faraday Trans. 1* **1984**, *80*, 2293.
(21) Truscott, T. G.; McLean, A. J.; Phillips, A. M. R.; Foulds, W. S. *Cancer Lett.* **1988**, *71*, 31.
(22) Firey, P. A.; Jones, J. W.; Jori, G.; Rodgers, M. A. J. *Photochem. Photobiol*. **1988**, *48*, 357.
(23) Hall, R. D.; Girotti, A. W. *Photochem. Photobiol.* **1988**, *47*, 795.
(24) Thomas, J. P.; Hall, R. D.; Girotti, A. W. *Cancer Lett.* **1987**, *35*, 295.
(25) Egorov, S. Y.; Kamalov, V. F.; Koroteev, N. I.; Krasnovsky, A. D.; Toleutaev, B. N.; Zinukov, S. V. *Chem Phys Lett.* **1989**, *163*, 421.
(26) Bohm, F.; Martson, G.; Truscott, T. G.; Wayne, R. P. *J. Chem. Soc., Faraday Trans.* **1994**, *90*, 2453.
(27) Kanofsky, J. R. *Photochem. Photobiol*. **1991**, *53*, 93.
(28) Baker, A.; Kanofsky, J. R. *Photochem. Photobiol*. **1993**, *57*, 720.
(29) Baker, A.; Kanofsky, J. R.; *Arch. Biochem. Biophys*. **1991**, *286*, 70.
(30) Bertoloni, G.; Salvato, B.; Dall'Acqua, M.; Vazzoler, M.; Jori, G. *Photochem. Photobiol.* **1984**, *39*, 811.
(31) Bertoloni, G.; Rossi, F.; Valduga, G.; Jori, G.; Van Lier, J. *FEMS Microbiol. Lett.* **1990**, *41*, 149.
(32) Nitzan, Y.; Gutterman, M.; Malik, Z.; Ehrenberg, B. *Photochem. Photobiol*. **1992**, *55*, 89.
(33) Wilson, M. personal communication.
(34) Jacob, H.−E. *Photochem. Photobiol.* **1974**, *19*, 133.
(35) Kjeldstad, B.; Christensen, T.; Johnson, J. *Photochem. Photobiophys*. **1986**, *10*, 163.
(36) Merchat, M.; Spikes, J. D.; Bertoloni, G.; Jori, G. *J. Photochem. Photobiol. B. Biol*. **1996**, *35*, 149.
(37) Burns, T.; Wilson, M.; Pearson, G. J. In *Proceedings of Photochemotherapy: Photodynamic Therapy and Other Modalities*; Ehrenberg, B., Jori, G., Moran, J., Eds.; SPIE Vol. 2625; SPIE: Washington, DC, 1996; p 288.
(38) Wilson, M.; Mia, N. *Lasers. Medical Sci*. **1994**, *9*, 105.
(39) Pottier, R.; Bonneau, R.; Joussot-Dubien, J. *Photochem. Photobiol*. **1976**, *22*, 59.
(40) Michaelis, L.; Granick, S. *J. Am. Chem. Soc*. **1945**, *67*, 1212.
(41) Fischer,H. *Z. Phys. Chem. Neue Folge* **1964**, *43*, 177.
(42) Grampp, G.; Hetz, G. *Ber. Bunsen-Ges. Phys. Chem*. **1992**, *96*, 198.
(43) Bonneau, R.; Fornier de Violet, P.; Joussot-Dubien, J. *Photochem., Photobiol*. **1974**, *19*, 129.
(44) Winter, G.; Shioyama, H.; Steiner, U. *Chem. Phys. Lett.* **1981**, *81*, 547.

(45) Pardekooper, M.; Van Gompel, A. E.; De Bont, H. J. G. M.; Nagelkerke, J. F.; Van Steveninck, J.; van Den Broek, P. J. A. *Photochem. Photobiol*. **1994**, *59*, 161.

(46) Beeby, A.; Bishop, S. M.; Meunier, H. G.; Simpson, M. S. C.; Phillips, D. In *Photodynamic Therapy and Biomedical Lasers*; Spinelli, P., Del Fante, M., Marchesini, R., Eds.; Elsevier: New York, 1992; p 732.

(47) Phillips, D. *Prog. React. Kinet.* **1997**, *22*, 175.

(48) Vincett, P. S.; Voigt, E. M.; Rieckhoff, K. E. *J. Chem. Phys.* **1971**, *55*, 4131.

(49) Ostler, R. B.; Scully, A. D.; Taylor, A. G.; Gould, I. R.; Smith, T. A.; Waite, A.; Phillips, D. *Photochem. Photobiol*. in press.

(50) Ostler, R. B. Ph.D. Thesis, University of London, 1988.

(51) Oldham, T. C. Ph.D. Thesis, University of London, 1996.

(52) Mack, J.; Stillman, M. J. *J. Am. Chem. Soc*. **1994**, *116*, 1292.

(53) Darwent, J. R.; McCubbin, I.; Phillips, D. *J. Chem. Soc., Faraday Trans. 2* **1982**, *78*, 347.

(54) Clack, D. W.; Yandle, Y. R. *Inorg. Chem*. **1972**, *11*, 1738.

(55) Davila, J.; Harriman, A. *Photochem. Photobiol*. **1989**, *50*, 29.

(56) Berinstain, A. B.; Scaiano, J. C.; Bohne, C.; Malenfant, P. R. L.; Sprott, G. D. *Photochem. Photobiol*. **1992**, *56*, 423.

(57) Minnocek, A.; Vernon, D. I.; Schofield, J.; Griffiths, J.; Parish, J. Howard; Brown, S. B. *J. Photochem., Photobiol. B. Biol*. **1996**, *32*, 159.

(58) Bertolini, G.; Reddi, E.; Gatta, M.; Barlini, C.; Jori, G. *J. Gen Microbiol*. **1989**, *135*, 957.

(59) Wilkinson, F.; Helman, W. P.; Ross, A. B. *J. Phys. Chem. Ref. Data* **1995**, *24*, 663.

(60) Gorman, A. A.; Rodgers, M. A. J. *J. Photochem. Photobiol. B: Biol*. **1992**, *14*, 159.

(61) Roberts, J. E.; Atherton, S. J.; Dillon, J. *Photochem. Photobiol*. **1991**, *54*, 855.

(62) Valduga, G.; Bertolini, G.; Reddi, E.; Jori, G. *J. Photochem. Photobiol. B: Biol.* **1993**, *21*, 81.

(63) Fischkoff, S.; Vanderkooi, J. M. *J. Gen. Physiol*. **1975**, *65*, 663.

(64) O'Loughlin, M. A. O.; Whillans, D. W.; Hunt, J. W. *Radiat. Res*. **1980**, *84*, 477.

(65) Pooler, J. P. *Photochem. Photobiol*. **1989**, *50*, 55.

(66) Oelckers, J.; Hanke, T.; Moser, J.; Rider, B. In *Photodynamic Therapy of Cancer* SPIE Proceedings 2078; SPIE: Washington, DC, 1994; p 116.

(67) Ito, I. *Photochem. Photobiol*. **1977**, *25*, 47.

(68) Pardekooper, M.; Gompel, A. E.; Van Steveninck, J.; Van Der Broek, P. J. A. *Photochem. Photobiol*. **1995**, *62*, 561.